DOT/FAA/AR-95/79

Office of Aviation Research
Washington, D.C. 20591

The Effect of Preloading on Fatigue Damage in Composite Structures: Part I

April 1996

Final Report

U.S. Department of Transportation
Federal Aviation Administration

NOTICE

Technical Report Documentation Page

1. Report No.	2. Government Accession No.	3. Recipient's Catalog No.
DOT/FAA/AR-95/79		

4. Title and Subtitle	5. Report Date
THE EFFECT OF PRELOADING ON FATIGUE DAMAGE IN COMPOSITE STRUCTURES: PART I	April 1996
	6. Performing Organization Code

7. Author(s)	8. Performing Organization Report No.
H. Thomas Hahn, Jeffrey L. Timmer, Jonthan Bartley-Cho, Seaman Lee, and Seung-Gyu Lim	

9. Performing Organization Name and Address	10. Work Unit No. (TRAIS)
Mechanical, Aerospace, and Nuclear Engineering Department Engineering IV UCLA Los Angeles, CA 90024-1597	11. Contract or Grant No. DTFA03-92-A-00003

12. Sponsoring Agency Name and Address	13. Type of Report and Period Covered
U.S. Department of Transportation Federal Aviation Administration Office of Aviation Research Washington, D.C. 20591	Final Report
	14. Sponsoring Agency Code AAR-431

15. Supplementary Notes

FAA Technical Monitors: Donald Oplinger
Peter Shyprykevich

16. Abstract

The effect of preload on damage development in unnotched graphite/epoxy laminates is studied. Two types of tension-tension fatigue tests were conducted on quasi-isotropic $[0/45/-45/90]_{S3}$, AS-4/3501-6 laminates, and damage was measured in the form of ply cracks. Baseline fatigue tests were run at constant amplitudes ranging from 20% to 60% of the ultimate tensile strength (UTS) while specimens with preloads of 50% to 80% UTS were tested in fatigue at the same amplitudes. The ply crack densities determined from edge replications in preloaded specimens were compared to those without preload. The effect of a preload on subsequent fatigue damage growth depended on the combination of both the preload level and the subsequent fatigue stress level. Since the tension preload was always higher than the tension-tension fatigue stress level, damage in preloaded specimens was more severe in the low-cycle region than nonpreloaded specimens. However, this preload-induced damage did not grow any more if the fatigue stress level was kept low. Preloads just above levels that cause significant damage (70% UTS and above here) appeared to retard fatigue damage development. At the highest tension-tension fatigue stress level of 40% UTS, the high-cycle damage in the form of matrix cracking rather decreased with increasing preload level. Thus, preloading could be beneficial at this stress level as far as the high-cycle ply crack damage is concerned.

17. Key Words	18. Distribution Statement
Preload, Fatigue, Graphite/Epoxy, Ply Crack, Crack Density	This document is available to the public through the National Technical Information Service, Springfield, Virginia 22161

19. Security Classif. (of this report)	20. Security Classif. (of this page)	21. No. of Pages	22. Price
Unclassified	Unclassified	44	

Form DOT F1700.7 (8-72) **Reproduction of completed page authorized**

TABLE OF CONTENTS

LIST OF FIGURES

LIST OF TABLES

EXECUTIVE SUMMARY

This report is the first of a series of reports that will provide comprehensive documentation of damage induced by spectrum fatigue loading in composite laminates. The overall study will systematically separate the loading environment into component parts to understand the interactions between each of the elements of the spectrum. Recorded here is the ply cracking of unnotched laminates due to five constant-amplitude tensile fatigue loads spaced within the likely design range. At each of these fatigue loads, the effect of a range of preloads on damage is assessed. The results for this simplest form of variable loading will be used as a building block to use with other data to eventually predict damage due to fatigue spectrum loading. This study is limited to damage effects on unnotched laminates under tensile loading; damage accumulation due to preloads and other spectrum components on open-holed and on impact damaged laminates under tension-compression and compression-compression loadings will be reported in the future. As this is the first report, a comprehensive bibliography is part of this report.

Two types of tension-tension fatigue tests were conducted on quasi-isotropic laminates and damage was measured in the form of ply cracks. Baseline fatigue tests were run at constant amplitudes ranging from 20% to 60% of the ultimate tensile strength (UTS) while specimens with preloads of 50% to 80% UTS were tested in fatigue at the same amplitudes. The ply crack densities determined from edge replications in preloaded specimens were compared to those without preload.

The effect of preloads on fatigue damage in composite laminates has been examined in order to better understand the modes of damage development and to assess the effect of proof testing. The effect of a preload on subsequent fatigue damage growth depended on the combination of both the preload level and the subsequent fatigue stress level. Since the tension preload was always higher than the tension-tension fatigue stress level, damage in preloaded specimens was more severe in the low-cycle region than nonpreloaded specimens. However, this preload-induced damage did not grow any more if the fatigue stress level was kept low. Preloads just above levels that cause significant damage (70% UTS and above here) appeared to retard fatigue damage development. At the highest tension-tension fatigue stress level of 40% UTS, the high-cycle damage in the form of matrix cracking rather decreased with increasing preload level. Thus, preloading could be beneficial at this stress level as far as the high-cycle ply crack damage is concerned.

1. INTRODUCTION.

Composite materials have been heralded as the material of the future for the last 20 years. Composites were supposed to replace traditional materials, mainly metallic materials, in many applications from aircraft to automobiles. The growth of composite use, however, has been much slower than originally predicted. Some of the reasons for the lack of use include high material cost, high production costs due to lack of automated manufacturing, and more complicated analysis. Another issue plaguing the industry, the one which will be addressed in this report, is the lack of an adequate understanding of long-term behavior. Confidence in long-term reliability must exist to use the inherent advantages of composite materials such as high specific strength and stiffness.

The behavior of composite structures under static and fatigue loads have been studied extensively, but is not as yet fully understood. The ultimate goal must be the ability to predict the long-term behavior of composite structures under any variable or spectrum loading conditions. The first step towards studying general spectrum loading is to determine the effect of proof testing on consequent fatigue behavior. Proof testing is a method of ascertaining the structural integrity by statically loading—i.e., proof loading—a structure to the design load or above before service. In composites, this static proof loading may produce damage in the form of ply cracking, which might not otherwise be present. Thus, it is important to find out how much damage is induced by proof loading and what effects this damage has on subsequent fatigue behavior. It is known that for metals, proof loading has beneficial effects on subsequent fatigue life and hence, unless it is representative of actual conditions, the proof loading is applied after fatigue cycles.

A test program was developed to determine the damage development due to fatigue and proof loads or preloads. Static tests were used to obtain material properties and constant-amplitude fatigue tests were used to define a baseline. Preloads were applied to test coupons which were then fatigued. Damage accumulation in the form of matrix cracks was monitored during these tests. Finally, the trends in damage accumulation due to the varying preloads and fatigue stresses were examined.

2. BACKGROUND.

Fatigue behavior of composite laminates has been studied by many researchers [1-7]. These researchers have studied many aspects of fatigue behavior which may be grouped into three basic ways to characterize fatigue effects on composite materials. The first is to use the method used for metals, namely the Strength-Life (S-N) curve which relates fatigue cycles to cyclic amplitude. The second method assumes that damage occurs and that the damage causes either the stiffness or the residual strength (post-fatigue static strength) of a laminate. Once the residual stiffness or strength is known, presumably, they can be related to remaining life. The third method is to investigate the actual damage occurring in a laminate. Once the types of damage that occur are determined, they can be related to loading and to remaining life. The damage can be characterized in terms of matrix cracking, longitudinal splitting, and delamination.

Popular topics of study include the effects of stacking sequence and laminate lay-up [8-12], frequency [13, 14], and type of loading [14-19] on fatigue behavior. In addition, a number of researchers [16, 20-25] have developed fatigue models based on residual strength and stiffness change. As a result, the modes of damage development are fairly well understood qualitatively. An understanding of these characterization methods used is useful in investigating preload effects.

2.1 GENERAL EFFECTS.

Early work on proof load effects in unidirectional composite coupons was done by Awerbuch and Hahn [1]. They determined that there is a relationship between the static strength and the fatigue life in a unidirectional composite. The exact nature of the relationship was not determined, however. Hahn and Kim [2] concluded that a relationship between static strength and fatigue life exists in unidirectional E-glass/epoxy composites. Using proof testing followed by fatigue cycling, they showed that failure occurred later in specimens with higher static strength.

As more researchers studied the damage development, the differences in damage due to static loading and fatigue loading became more apparent. Mar [3] concluded that damage modes under static load cannot be used as models for damage initiation or propagation under cyclic loads. He suggested that research emphasis should be on propagation of damage under cyclic loads. Razvan et al. [4] found that the type of damage incurred during fatigue was not affected by the fatigue load level, but the interaction between damage modes was important. The difference in interaction of damage modes suggests that damage accumulation in composite structures is dependent on load history.

As constant amplitude loading was not representative of actual service load, emphasis was soon placed on the effects of random or spectrum loads. Cumulative damage due to varying fatigue loads was studied by Hwang and Han [5]. They developed models using fatigue modulus and resultant strain as damage indicators. The results of their investigation implied that significant effort was yet needed for a realistic fatigue model. A concept of "characteristic damage state" was suggested by Masters and Reifsnider [6]. The idea was that regardless of previous loading conditions, the damage state of a quasi-isotropic composite will saturate at the same level. In their studies, damage was measured in terms of matrix crack spacing which stopped decreasing at the same level regardless of loading history. Reifsnider [26] used this characteristic damage state in his "critical element concept" model for life prediction. The "critical element concept" was an approach to quantitatively analyze and predict the strength reduction associated with damage accumulation. The concept used critical elements of characteristic damage states to predict life. Tension-tension and tension-compression specimens were used to illustrate application of the idea.

Rotem and Nelson [27] conducted tests in which tension-compression (T-C) fatigue behavior was compared to tension-tension (T-T) and compression-compression (C-C) behavior. Tension-compression behavior was found to be the severest loading case as either tension or compression failure can occur. A fatigue failure envelope was proposed and demonstrated. Wolterman,

Kennedy, and Farley [28] also conducted T-T, T-C, and C-C tests in addition to quasi-static tests to assess their effects on thick cross-ply laminates with both brittle and tough matrix and stitched composites with a hole. The tough matrix developed less damage and the unstitched one developed less longitudinal damage but more transverse damage. The residual strength was affected by the matrix material and the damage state.

Tension-tension fatigue of quasi-isotropic composite cylinders was found to be comparable to similar fatigue in composite coupons by Norman, Civelek, and Prucz [29]. Although the ultimate strengths of coupons and cylinders were different, the fatigue lives at the same percentage of ultimate tensile strength (UTS) are very similar. Notched and unnotched laminates were compared under fatigue conditions by Xiao and Bathias [8]. Although the fatigue strengths of the two types of laminates were different, the ratios of the fatigue strength to UTS were the same. Orthotropic and quasi-isotropic laminates were also compared and similar results occurred.

2.2 RESIDUAL STRENGTH AND STIFFNESS REDUCTION.

A popular method of representing damage in composites during fatigue is by stiffness reduction. The idea is that as damage occurs in individual plies, they lose some of their load carrying capabilities and stiffness, resulting in lower residual strength and overall stiffness. Because changes in stiffness can be relatively easily measured by nondestructive methods, it can be an effective tool in determining the life of a composite laminate.

A large number of stiffness reduction models have been developed [16, 20-25]. They generally assume that stiffness is a measure of damage and that it can be related to residual strength and remaining life. The mechanics of fatigue damage were developed by Poursartip, Ashby, and Beaumont [21]. They modeled the damage growth rate as a power function of the stress amplitude and the mean stress. Other models include Whitworth [22], who based his model on fatigue tests conducted on graphite/epoxy $[\pm 35]_{2s}$ laminates. The model is restricted to constant-amplitude fatigue and a reasonable fit was found. Jen et al. [24] modeled modulus degradation in quasi-isotropic laminates subjected to tension-tension fatigue. Liu and Lessard [25] assumed that residual stiffness is a function of matrix crack density and delamination area. Based on this assumption, they proposed a model whose parameters can be found from testing of cross-ply laminates. Giavotto et al. [16] studied the effects of stress ratio, variable amplitude loading, and some changes in load spectrum. Stiffness variations were also correlated with damage growth. Antibuckling guides were found to significantly influence damage onset and growth for compression and fatigue limits load level below which there were damage occurrences. In a series of four papers, Spearing et al. [30-33] observed notch tip damage, developed a fatigue model for growth of that damage, extended the model to predict post fatigue residual notch strength, and finally developed a stiffness degradation model.

A new concept in the form of the "fatigue modulus" was defined by Hwang and Han [34] and was used to model the damage development in composite laminates. Fatigue modulus is defined as the slope of the applied stress and resultant strain at a specific cycle. A theoretical equation was determined to predict fatigue life using fatigue modulus and its degradation. A strain failure

criterion was used. Lee et al. [20] also used the fatigue modulus in their formulation of a degradation model. A reasonable correlation was obtained when the model was applied to a matrix dominated $[\pm 45]_{2s}$ laminate. Tsai, Doyle, and Sun [14] correlated the effect of frequency on fatigue life with a model using dynamic modulus as a damage indicator.

While many researchers studied the relationship between residual stiffness and fatigue life, still many others often tried to correlate residual strength with fatigue cycles. One of the early residual strength models was proposed by Yang [35] after observing that the ultimate tensile strength of an unnotched unidirectional specimen appeared to decrease monotonically with the number of load cycles. He also observed that a proof load could be used to test the remaining fatigue life of a part by comparing the proof stress to the predicted residual strength. While only limited testing was done, Radhakrishnan [18] later independently verified Yang's model with his own tests. Radhakrishnan's model predicted with reasonable accuracy the minimum number of fatigue cycles a specimen will survive after it has been proof tested to a certain level. Yang and Du [19] further modified Yang's [35] original constant-amplitude residual strength model to account for in-service loading spectra. A two-parameter Weibull distribution was used and showed good correlation with unidirectional unnotched composite laminates and composite-to-titanium bolted joints. Yang et al. [23] made further modification to his model and derived a linear regression model based on a Bayesian approach.

2.3 DAMAGE ACCUMULATION.

A thorough understanding of damage development is essential in the determination of fatigue characteristics in composite materials. This has prompted many experimental investigations of damage in composites of many configurations and under a variety of loading conditions. Because of these investigations, the qualitative progression of damage is fairly well known. The typical damage sequence in multidirectional laminates subjected to tensile fatigue is first by ply cracking of off-axis plies, followed by edge delaminations, followed by fiber fracture, leading to final failure.

The surface and internal damage observations are accomplished through several appropriate nondestructive evaluation (NDE) techniques. A very useful paper written by Stinchcomb [7] gives insight into the pros and cons of tracking the damage accumulation in composite specimens by variety of NDE techniques. Edge replication and microscopy allow simple and accurate analysis of surface features, but do not allow damage information through the width of the coupon. X-ray radiography and ultrasonic methods allow inspection of the interior, but lack in resolution. Thermography and stiffness changes were also used to estimate damage, but do not give information on any specific damage modes.

Even with an appropriate damage monitoring technique, damage tracking is made difficult by the anisotropic nature of composite materials. Unlike traditional isotropic materials, composite materials have properties that are tailorable. While this is very useful for providing an efficient structure, each change in lay-up or stacking sequence gives different damage accumulation characteristics. Realizing this, various investigators [8-12] have examined the effect of changing the laminate stacking sequence. Ratwani and Kan [11] observed that both damage development

and final failure mode changed with stress ratio (R = 0.1 and R = ∞) and stacking sequence. Delamination and matrix cracking appeared at locations of highest interlaminar or normal stress. Masters and Reifsnider [6] also found that matrix crack, longitudinal cracks, and delamination developed differently in $[0/\pm45/90]_s$ and $[0/90/\pm45]_s$ laminates. Saturation crack spacing was different for each type of laminate. Based on this observation, a characteristic damage state was suggested which was dependent on the laminate lay-up. Kim and Aoki [9] studied the effect of load types (static and fatigue), ply thickness, and laminate sequence. They tested several quasi-isotropic laminates of two basic configurations but containing 90° plies of various thickness: $[0/\pm45/90n]_s$ and $[0/90n/\pm45]_s$ n=1,3,6. When tension was applied to the specimens, the former lay-up was found to produce tensile interlaminar normal stress along the free edges while the latter produced compressive stresses. Under static load, the tensile stress resulted in delamination for that laminate. However, while no delamination occurred for the lay-up with compressive interlaminar stress under static load, extensive delamination occurred during tensile fatigue following transverse ply cracks, indicating a strong interaction between the two damage modes. Importantly, they observed a ply thickness effect on the initiation and accumulation of transverse ply cracks. Load level and number of cycles required to initiate ply cracking decreased with increasing ply thickness. As for crack accumulation, increasing the ply thickness decreased crack density. Harrison and Bader [10] observed a similar thickness effect. Tests conducted on [0/90/0] and [±45] lay-ups revealed that ply cracking initiation strain increased with thinner plies. They also observed that ply cracking strain for [0/90/0] lay-up was lower in fatigue than in uniaxial static tension. Lafarie-Frenot and Henaff-Gardin [12] also described ply thickness variation effects on fatigue mechanisms of matrix cracking. Two cross-ply lay-ups, $[0_3/90/0_4]_s$ and $[0_7/90]_s$, were tested in tension-tension. Both edge cracks and their widthwise extension were monitored, enabling them to deduce the crack surface growth data. They concluded that, as far as ply cracking was concerned, thinner plies exhibited higher cracking resistance. The thinner plies delayed the onset of ply cracks, lowered the crack surface growth rate, and resulted in a smaller saturation crack surface area.

Having understood the progression of damage qualitatively, researchers began developing models to predict damage in a quantitative manner. Many of the models follow the stiffness reduction models closely and attempt to relate stiffness change and damage (crack density). Badaliance and Dill [17] formulated a model based on an experimentally observed fatigue damage mechanism and a damage parameter based on intralaminar resin cracking. Spectrum life was predicted using a damage mechanism and a linear residual strength reduction fatigue damage model. The accuracy of the spectrum life prediction depended on the validity of the residual strength reduction model. Stiffness reduction was shown to be directly proportional to crack density in $[0/90]_s$ fiberglass by Ogin et al. [36]. Their fatigue model showed good agreement with experimental stiffness reduction curves.

Radakrishnan [18] developed a unidirectional tension-tension residual strength model for unnotched unidirectional graphite epoxy laminates. Effect of preload was also considered and found to be consistent with Yang's model [35]. A damage model which took into account static loadings and includes internal loadings was formulated by Thionnet and Renard [37]. The model assumed that cracks appear the same way under both static and fatigue loading. Fatigue matrix cracking and the subsequent stiffness reduction in matrix dominated $[+45/-45]_{2s}$

laminates were correlated with a fatigue modulus degradation model by Lee et al. [20]. A reasonable correlation between predicted fatigue life distributions and experimental results was obtained. Gamby [38] recently proposed a numerical model for the accumulation of transverse cracks in a composite laminate subjected to tensile fatigue loading. He found that his damage growth rate equation predicted transverse ply cracking as long as it was the only damage accumulation mechanism.

Carlsson et al. [15] tested quasi-isotropic 32-ply graphite/epoxy specimens in static tension and tension fatigue, some with preload and some with moisture. The first damage found was transverse 90° matrix cracking, which then moved into -45° plies upon increased loading and cycles. No delamination was seen under static load conditions. Preloads caused earlier delamination due to increased matrix cracking while moisture was found to delay damage development. The leveling off of the crack density at a particular plateau with increasing fatigue cycles, known as the characteristic damage state, was also observed. A fatigue failure envelope was proposed and demonstrated. Lee and De Charantenay [39] observed that fatigue damage development was accelerated under long hold time and high fatigue stress levels. The main cause of the acceleration was the damage produced by the hold time loading itself. They also observed that at shorter hold time and lower fatigue stress levels the fatigue damage development was retarded. They stated that the reason for the retardation effect is the "pronounced plastification at the crack tip of damage and the reduced mean load level of subsequent fatigue loading after the holding times."

To summarize, initially researchers trying to determine the fatigue life of composites attempted to use the S-N curves used for metals. These curves were found to be too general to cope with the anisotropic nature and changing lay-up in composites. Further research showed that the stiffness and the residual strength of composite laminates degraded during fatigue, leading to the assumption that fatigue life can be predicted by monitoring the residual properties. Models were developed which could predict the stiffness change, residual strength change, and life of a part for certain simple laminates. However, the total stiffness change over the life of a part is relatively small, making its measurement difficult. In addition, both stiffness and residual strength degradation is a secondary effect of the actual damage occurring within the laminate. To really understand how fatigue affects composites, the actual damage within the laminate, including ply cracks and delamination, must be studied. Damage of this type due to constant-amplitude fatigue has been examined to the extent that the modes of damage development are well documented. However, no one has determined the effect of a variable loading environment (spectrum loading) on damage development within the laminate.

The first step towards finding damage development due to spectrum loading is to perform a systematic study breaking the loading environment into component parts to understand the interactions between each of the elements of the spectrum. In this report, the first portion of that step has been examined. A systematic study investigating ply crack damage development over a range of constant-amplitude fatigue loading was undertaken. At each of these load amplitudes a range of preloads was applied. The types of damage induced by preloading were identified and the way this initial damage changes the subsequent fatigue damage growth were shown. The

study, however, is limited to subcritical damage—i.e., ply cracking—only, excluding the edge damage and final failure of the specimens.

3. EXPERIMENTAL PROCEDURE.

Static tensile tests were performed to determine the mechanical properties of coupons used for testing. Three additional static tests were performed while measuring crack density to assess damage during static loading. Baseline fatigue tests were performed at a constant stress amplitude with a stress ratio ($R = \sigma_{min}/\sigma_{max}$) of 0.1. These baseline tests were performed in 10% increments from 20% to 60% of the ultimate tensile strength (UTS). To gauge the effects of preloading, specimens were loaded from 50% to 80% UTS before being fatigued. The preloads were applied at the rate of 0.1 hertz (R=0). All subsequent fatigue cycles had a sinusoidal loading rate of 10 hertz. The ply crack densities were periodically measured at the edge during the fatigue tests. The test matrix used is shown in table 1.

3.1 SPECIMEN PREPARATION.

The material system used was Hercules AS4/3501-6 graphite/epoxy. The laminate lay-up was quasi-isotropic $[0/45/-45/90]_{S3}$ making a total of 24 plies. AS4/3501-6 was chosen because of its widespread use in the aircraft industry. Similarly, a quasi-isotropic lay-up was selected because of its common use.

All laminate fabrication was performed at the Pennsylvania State University. Square panels 61 by 61 cm were fabricated in an autoclave at Pennsylvania State University following the manufacturer's suggested cure cycle. These panels were cut into six subpanels 20.3 cm wide by 30.48 cm long. The subpanels were then C-scanned to check for any gross defects or delaminations. The subpanels were then shipped to the University of California, Los Angeles, where all further preparation and testing took place.

To make the test coupons, the subpanels were cut with an abrasive diamond saw (180 grit) into 20.3 by 2.54 cm coupons, carefully avoiding process defects detected by the C-scans. One of the specimen edges was then sanded to 800 grit to facilitate monitoring of damage growth. An ultrasonic bath was used to remove debris from the cut and sanded edges.

3.2 TEST PROCEDURE.

For improved gripping, the last 6.35 cm section at each end of the specimen was roughed to 220-320 grit. The end tabs used to prevent fiber breakage during gripping were 0.32-cm-thick 6061 aluminum with dimensions of 6.67 by 2.54 cm. The edges that would contact the gage section were rounded to a 1.5 mm radius to reduce any stress concentration. The inside edge of the end tab was bead blasted and left untouched before attaching to the specimen (no adhesive was used). The tabs were held in place at the proper gage length of 7.62 cm using an ordinary masking tape along the sides of the specimen and the tabs. This method allowed the tabs to be secured before gripping.

All tests were performed on an MTS 22 Kips servohydraulic testing machine. The grips utilized were hydraulic with 5.08-cm-wide by 7.62-cm-high jaws as seen in the fixture shown in figure 1. To reduce the force on the corner of the end tabs, 0.32 cm of the tab was left ungripped. This configuration yielded the desired 7.62-cm gage length. The specimen and tabs were aligned in the grip using previously aligned stops bolted to the grip jaws. The hydraulic grips were then slowly closed, first on the bottom jaw enough to hold the specimen and then both jaws were closed simultaneously. The pressure in the grips was brought to 7.5 KPa for fatigue tests and 12.4 KPa for static tests.

All testing was conducted at ambient laboratory conditions. Five static tensile tests were performed to evaluate the material properties, including tensile stiffness and ultimate tensile strength (UTS). These tests were performed at 0.077 cm/minute in accordance with ASTM D3039 standard. Strain was measured using Micromeasurements' axial strain gages mounted to the center of one side of the specimen along the 0° direction.

3.3 REPLICATION PROCEDURE.

A replicating tape (Ladd, Inc.) was found to be both effective and convenient to monitor damage. The tape is an acetate strip which is softened with acetone and applied with light pressure to the specimen edge while under load where it is allowed to dry for 5 minutes. The result is an inverted replica of the edge on which damage can easily be viewed using a light microscope.

The observed damage was mostly in the form of cracks within off-axis plies of the same orientation as seen in the photograph in figure 2. The cracks in each ply were counted from the replica over a 12.7 mm length on a light microscope. Only cracks extending through the entire ply thickness were counted. In the case of the two adjacent 90° plies, only cracks through both 90's were counted. The data were then quantified in terms of a crack density which was defined as the number of cracks in a group of contiguous plies with the same orientation per unit length of the laminate (no. of ply cracks/cm). Figure 3 shows how individual plies were identified. The plies were numbered from the middle ($Z = \pm 1$) toward the outer plies ($Z = \pm 12$). Crack densities were averaged over each symmetric pair of ($\pm Z$) plies.

During the static test, the crosshead was stopped periodically for five minutes while an edge replication was taken. After the replication the original speed was resumed until the next replication stress level was reached and another replication was taken. Two of the three static tests had a total of 16 replicas while the third had 8 replicas. The load histories of each of these specimens including hold time during replication are shown in figure 4.

In fatigue, cycling was stopped intermittently to allow edge replication. All replicas were taken while under tensile stress to open the cracks and allow the acetate solution to seep in. At fatigue stresses of 30% UTS and higher, the stress during replication was 30% UTS.

4. RESULTS AND DISCUSSION.

4.1 STATIC TENSILE TEST RESULTS.

The specimens tested quasi-statically had an average ultimate tensile strength (UTS) of 747 MPa and an average longitudinal Young's modulus (E_x) of 55.1 GPa. The strain at failure for all tests was in the vicinity of 14,000 microstrain (see table 2). An example of a stress-strain curve generated by the static tests is shown in figure 5.

From the edge replicas of the three static test specimens, the first damage identified at the specimen edges was the cracking of the 90° plies. Ply cracks as defined here consist of matrix/interface failure in the off-axis plies. When cracks appeared, they propagated immediately through the entire thickness of both 90° plies and were arrested at the -45° interfaces. More cracks appeared in 90° plies as the applied stress increased. As shown in the micrograph in figure 2, -45° ply cracks first appeared at either end of the 90° ply cracks. No cracks in +45° plies were visible during static tension nor was any delamination evident.

In specimens with 16 replications, the first cracks appeared at 28% UTS in all three sets of 90° plies (see figures 6 and 7). The load histories of these two specimens are shown in figure 4. The cracks in the 90° plies multiplied as the stress increased. At 44% UTS, the -45° plies began to crack. During the last replication before failure (96% UTS) the crack densities in the outside 90° plies ($Z = \pm 8,9$) averaged 17.3 cracks/cm and those in the middle 90° plies ($Z = \pm 1$) averaged 20.0 cracks/cm. In contrast, the specimen with a total of 8 replications shown in figure 8 yielded crack densities at 96% UTS of only 13.4 cracks/cm for the outside 90° plies ($Z = \pm 8,9$) and 15.0 for the middle 90° plies ($Z = \pm 1$). In addition, first ply cracking occurred at 40% UTS for the 90° plies and 64% for the -45° plies.

There are several possible reasons for the differences between these specimens. The first is of course the variability from specimen to specimen as crack densities show a large scatter. The second reason is that ply cracking may not be solely a function of the applied stress but also of load history. Loading of specimens with 16 replications was interrupted more often than that of specimen 3, effectively increasing the time under load as seen in figure 4. More frequent replications and time under load seem to increase the crack densities in coupons held at the same stress level. Lee and De Charentenay [39] described similar fatigue acceleration effects due to high peak loads. The third possible reason for variability is the possibility of deleterious effects from the acetone that was used in replication. According to Favre and Laizet [40], stress corrosion cracking due to acetone in X-ray enhancing solution can occur in composite fatigue specimens. To determine the extent, if any, of this phenomenon, the crack densities in two specimens fatigued to one million cycles were compared. One specimen had approximately 15 replications taken under load during its testing period, while the other was untouched by replications and acetone. Results indicated that the replications did not significantly increase the crack densities.

4.2 FIRST-CYCLE CRACK DENSITIES.

Figures 9 and 10 illustrate the crack densities generated after the first cycle of fatigue loading or preload. The 90° plies are shown in figure 9 while the -45° plies are seen in figure 10. The first fatigue cycle was conducted at 0.1 Hz although the subsequent cycling after replication was conducted at 10 Hz. More data points are seen at higher stresses because preload specimens are included. As in the static load case, cracking appears first in the 90° plies. The inner 90° plies ($Z = \pm 1$) tended to crack before the outer 90° plies ($Z = \pm 8,9$). Once the 90° ply cracking was saturated, the cracks propagated into the -45° plies. As in the 90° plies, the middle -45° plies ($Z = \pm 2$) cracked before the outer plies. No cracks were found in +45° plies during first-cycle loads, just as in the static case.

Applying a preload to a specimen is very similar to applying loads during quasi-static tensile testing, the only difference being the rate at which the load is applied and the time the load is held (see load histories, figure 4). Therefore, at the same applied stress level, the crack densities after the first fatigue cycle preload should be the same as those in static tension if there is no effect of loading rate or hold time. From the two sets of graphs in figures 6 to 8 (static test results) and in figures 9 and 10 (preload results), it is seen that in static tension, cracks appear earlier and multiply more quickly than during the first fatigue cycle or preload. This observation is in agreement with the earlier discussion on the effect of the replication frequency.

4.3 CONSTANT-AMPLITUDE FATIGUE.

Ply crack density growth versus fatigue cycles at constant amplitude of 20%, 30%, 40%, 50%, and 60% UTS are shown in figures 11 to 15, respectively. The fatigue ply cracking follows the same pattern as static ply cracking. The progression is as follows; the middle 90° plies ($Z = \pm 1$) crack, then the outer 90° plies ($Z = \pm 8,9$), followed by the middle -45° plies ($Z = \pm 2$), and finally the outer -45° plies ($Z = \pm 7$). Differences, though, begin to occur at high fatigue cycles under high-amplitude fatigue load.

Longitudinal cracking occurs in the 90° plies and delaminations begin to grow at the -45/90 interfaces. These delaminations tend to grow where a 90° horizontal ply crack has stopped at a -45° ply. In addition, at high fatigue stress levels (40% UTS and greater) and high fatigue cycles (500,000+), cracks begin to appear and propagate in the +45° plies. The number of these cracks is minimal and scattered; therefore, they were not included in the crack density measurements.

At 20% constant-amplitude fatigue, a very small number of ply cracks are initiated and these only at high fatigue cycles (200,000+). A threshold stress level at which fatigue cracking becomes significant appears to exist between 20% and 30% UTS constant-amplitude fatigue. While 20% loading produces very little crack damage, even at high cycles, 30% UTS loading produces significant amounts of cracking, especially at fatigue cycles on the order of 10^6. The initial cycles at 30% UTS produce a few cracks which multiply steadily, particularly in the 90° plies, as cycles increase. The -45° ply cracks begin to appear at approximately 10,000 cycles and multiply in an approximately logarithmic fashion. The 90° ply crack densities level off after

about 100,000 cycles at the saturation level, the phenomena described by Masters and Reifsnider [6]. The -45° ply cracking did not appear to saturate, but continued to increase until the tests were stopped at 10^6 cycles.

Forty percent constant-amplitude fatigue produces cracking which is approximately linear on a log scale in both 90° and -45° plies. The 90° plies begin cracking immediately and progress to just under 20 cracks/cm at close to 300,000 cycles where saturation occurs. The -45° plies start cracking later at about 1,000 cycles but increase more quickly to 20 cracks/cm at 10^6 cycles but do not saturate at that time. Forty percent UTS constant-amplitude fatigue is the first level at which +45° ply cracks are seen to initiate and multiply.

At 50% UTS constant-amplitude fatigue and higher stresses, cracks initiate in the first cycle and quickly grow to saturation levels, figure 14. At that point, damage phenomena other than ply cracking, such as longitudinal splitting and delamination, takes over and grows. At 60% UTS constant-amplitude fatigue, the specimens do not reach the 10^6 cycle cutoff level before delaminations completely destroy the integrity of the coupons (figure 15).

4.4 CONSTANT-AMPLITUDE FATIGUE WITH PRELOADS.

The effect of preload on subsequent fatigue ply crack growth is shown in figures 16 to 27. These figures show ply crack density data taken during tests with preloads ranging from 50% to 80% UTS and fatigue stress amplitudes from 20% to 40% UTS.

The 50% UTS preload, figures 16 to 18, does not induce much ply cracking and does not appear to produce more damage than specimens without preloads. In fact, such a low preload appears to reduce the subsequent damage growth compared to nonpreloaded specimens when the fatigue stress levels are 30% UTS or higher. Although this conclusion awaits further corroboration, one can safely say that the 50% preload has no harmful effect on subsequent fatigue.

At 60% preloads as seen in figures 19 to 21, considerable ply cracking damage occurs during the preload cycle. At a low cyclic amplitude (20% UTS), very little additional cracking occurs during fatigue. At high cyclic stresses (30% and 40% UTS), however, fatigue damage starts immediately and increases to the saturation level before 200,000 cycles have been reached.

Even more cracking occurs during the 70% preload (see figures 22 to 24). The damage accumulation does not continue after the preload until the high-cycle range (200,000+) has been reached for any of the cyclic amplitudes. The damage then grows steadily until the cutoff level (10^6 cycles) has been reached.

Finally, at 80% UTS preload, virtually all of the ply cracking occurs during the preload. This can be seen in figures 25 to 27 where there is very little difference between the first and millionth cycle crack densities. Only at high amplitude fatigue (40% UTS) does significant cracking occur after the preload.

The results in figures 16 to 27 can be summarized as follows. As the preload increases, the resulting ply cracking is more severe. If the preload damage is more severe than the fatigue damage without preload, then there is no damage growth in subsequent fatigue. Otherwise, there will be damage growth in subsequent fatigue. However, the resulting high-cycle damage is still the same as the corresponding fatigue damage without preload. The effect of the preload before constant-amplitude fatigue is shown in figures 28 to 33. The figures are grouped by ply number and show the crack density as measured immediately after each preload and after 10^6 fatigue cycles. Figures 28 and 29 show the effect of varying preload on the damage accumulation from 20% constant-amplitude fatigue in 90° and -45° plies. As the preload increases, the 90° ply crack densities at 1 and 10^6 cycles increase in a linear fashion. Little fatigue effect (crack density growth after preload) is evident at 20% constant-amplitude fatigue. The crack density trends in the -45° plies are very similar to that of the 90° plies, with slightly lower crack densities. The 90° ply crack densities range from 0 cracks/cm at 50% preload to approximately 12 cracks/cm at 80%. While the -45° ply crack densities range from 0 cracks/cm at 50% to about 9 cracks/cm at 80%.

At the medium fatigue stress level of 30% UTS, the preload begins to have less of an effect on the 10^6 cycle crack density. Preloading to 50% and 60% UTS increases the subsequent fatigue damage as shown in figures 30 and 31. However, this deleterious effect disappears as the preload is increased further to 80% UTS.

At 40% constant-amplitude fatigue with a 70% UTS preload, the ply cracking at low-cycle fatigue is less than with 80% preload, but at 10^6 cycles the ply cracking levels with and without preload are very similar as seen in figures 32 and 33. The most interesting effect of preload is seen at the high fatigue stress level of 40% UTS. In this case, preloading appears to decrease the amount of final damage.

The effects of preload can be summarized as follows. At 20% UTS fatigue, little significant ply cracking occurs. A threshold between 20% and 30% UTS fatigue appears to exist for significant damage accumulation during constant-amplitude fatigue. At high cycles during 30% and 40% UTS fatigue, large numbers of cracks and eventually delaminations occur. Adding preloads of 50% to any of these three fatigue loadings does little to affect damage accumulation, except at 40% UTS fatigue, where it appears to lower slightly the ply crack density at one million cycles. Increasing the preload to 60%, 70%, and 80% increases low-cycle damage but reduces the damage induced by fatigue at higher cycles.

The preloads introduced here are similar to the hold-time stresses used by Lee and De Charantenay [39]. If their data and the data shown here are compared, similar phenomena are seen. Long hold-time stresses accelerate damage development as do high preloads. At shorter hold-time stresses fatigue damage is retarded. They state that the reason for the retardation effect is from "pronounced plastification at the crack tip and the reduced mean load level of subsequent fatigue loading after the holding times." If it is true, this observation may explain why during tests with 50% preloads the subsequent fatigue damage appears less than in tests without the preload.

5. CONCLUSIONS.

The contribution of this report is to provide the first step towards the comprehensive documentation of damage induced by spectrum fatigue loading. Recorded here is the ply cracking due to five constant-amplitude fatigue loads spaced within the likely design range. At three of these constant-amplitude fatigue loads, the effect of preloads on damage is assessed, giving results for the simplest form of variable loading. The results can be used as a building block to use with other data to eventually predict damage due to spectrum fatigue loading.

The effect of preload on subsequent fatigue damage growth depends on the combination of both the preload level and the subsequent fatigue stress level. Since the preload is higher than the fatigue stress level, the resulting damage in the low-cycle region is more severe. The preload-induced damage did not grow any more if the fatigue stress level was kept low. Preloads which are just above levels which cause significant damage (70% UTS and above here) appear to retard fatigue damage development. At the highest fatigue stress level of 40% UTS employed in the present work, the high-cycle damage rather decreases with increasing preload level. Thus, preloading would be beneficial at this stress level as far as the high-cycle damage is concerned. In any case, based on today's design strains, the effect of preload on fatigue damage is not significant and preload can be applied before or after fatigue loading.

Ply cracking is time dependent and hence crack densities measured depend on load histories of the specimen. Another complicating factor that has to be reconciled in data analysis is the sensitivity of ply cracking to specimen variability. Both factors make it difficult to compare data obtained from different specimens. Yet the trends are clear from the data generated.

6. REFERENCES.

1. Awerbuch, J. and Hahn, H.T., "Fatigue and Proof Testing of Unidirectional Graphite/Epoxy Composite," Fatigue of Filamentary Composite Materials, ASTM STP 636, K.L. Reifsnider and K.N. Lauraitis, Eds., American Society for Testing and Materials, 1977, pp. 248-266.

2. Hahn, H.T. and Kim, R.Y., "Proof Testing of Composite Materials," *Journal of Composite Materials*, Vol. 9, July 1975, pp. 297-311.

3. Mar, J.M., "Fracture, Longevity, and Damage Tolerance of Graphite/Epoxy Filamentary Composite Material," *Journal of Aircraft*, Vol. 21, No. 1, January 1984, pp. 77-83.

4. Razvan, A., Bakis, C.E., Wagneiz, L., and Reifsnider, K.L., "Influence of Cyclic Load Amplitude on Damage Accumulation and Fracture of Composite Laminates," *Journal of Composites Technology and Research*, Vol. 10 No. 1, Spring 1988.

5. Hwang, W. and Han, K.S., "Cumulative Damage Models and Multi-Stress Fatigue Life Prediction," *Journal of Composite Materials*, Vol. 20, March 1986, pp. 125-151.

6. Masters, J.E. and Reifsnider, K.L., "An Investigation of Cumulative Damage Development in Quasi-Isotropic Graphite/Epoxy Laminates," Damage in Composite Materials, ASTM STP 775, K.L. Reifsnider, Ed., American Society for Testing and Materials, Philadelphia, 1988, pp. 40-62.

7. Stinchcomb, W.W., "Nondestructive Evaluation of Damage Accumulation Processes in Composite Laminates," *Composites Science and Technology*, Vol. 25, No. 2, 1986, pp. 103-118.

8. Xiao, J. and C. Bathias, "Fatigue Behavior of Unnotched and Notched Woven Glass/Epoxy Laminates," *Composites Science and Technology*, Vol. 50, pp. 141-148, 1994.

9. Kim, R.Y. and R. M. Aoki, "Transverse Cracking and Delamination in Composite Materials," *Fibre Science and Technology*, Vol. 18, pp. 203-216, 1983.

10. Harrison, R.P. and M. G. Bader, "Damage Development in CFRP Laminate under Monotonic and Cyclic Stressing," *Fibre Science and Technology*, Vol. 18, pp. 163-180, 1983.

11. Ratwani, M.M. and H. P. Kan, "Effect of Stacking Sequence on Damage Propagation and Failure Modes in Composite Laminates," Damage in Composite Material, ASTM STP 775, K.L Reifsnider, Ed., American Society for Testing and Materials, 1982, pp. 211-228.

12. Lafarie-Frenot, M.C. and C. Henaff-Gardin, "Formation and Growth of 90° Ply Fatigue Cracks in Carbon/Epoxy Laminates," *Composites Science and Technology*, Vol. 40, pp. 307-326, 1990.

13. Rotem, A, "Load Frequency Effect on the Fatigue Strength of Isotropic Laminates," *Composites Science and Technology*, Vol. 46, pp. 129-138, 1993.

14. Tsai, G. C., J. F. Doyle and C. T. Sun, "Frequency Effects on the Fatigue Life and Damage of Graphite/Epoxy Composites," *Journal of Composite Materials*, Vol. 21, pp. 2-13, 1987.

15. Carlsson, L., C. Eidefeldt and T. Mohlin, "Influence of Sublaminate Cracks on the Tension Fatigue Behavior of a Graphite/Epoxy Laminate," Composite Materials: Fatigue and Fracture, ASTM STP 907, H. T. Hahn, Ed., American Society for Testing and Materials, Philadelphia, 1986, pp. 361-382.

16. Giavotto, V., G. Sala, L. Lazzeri, G. Zhentong, Z. Gong-xing and Y. Nai-Bin, "Damage Growth under Constant and Variable Amplitude Loading," 7th ICCM, Vol. 3, 1989.

17. Badaliance, R. and H. D. Dill, "Damage Mechanism and Life Prediction of Graphite/Epoxy Composites," Damage in Composite Material, ASTM STP 775, K.L Reifsnider, Ed., American Society for Testing and Materials, 1982, pp. 229-242.

18. Radhakrishnan, K., "Fatigue and Reliability Evaluation of Unnotched Carbon Epoxy Laminates," *Journal of Composite Materials*, Vol.18, pp. 21-31, 1984.

19. Yang, J.N. and S. Du, "An Exploratory Study into the Fatigue of Composites Under Spectrum Loading," *Journal of Composite Materials*, Vol. 17, pp.511-526, 1983.

20. Lee. L. J., J. N. Yang and D. Y. Sheu, "Prediction of Fatigue Life for Matrix Dominated Composite Laminates," *Composites Science and Technology*, Vol. 46, pp. 21-28, 1993.

21. Poursartip, A., M. F. Ashby and P. W. R. Beaumont, "Fatigue Damage Mechanics of a Carbon Fiber Composite Laminate. I: Development of a Model," *Composites Science and Technology*, Vol. 25, pp. 193-218, 1986.

22. Whitworth, H. A., "Modeling of Stiffness Reduction of Graphite/Epoxy Composite Laminates," *Journal of Composite Materials*, Vol. 21, pp. 362-372, 1987.

23. Yang, J. N., D. L. Jones, S. H. Yang and A. Meskini, "A Stiffness Degradation Model for Graphite/Epoxy Laminates," *Journal of Composite Materials*, Vol. 24, pp. 753-769, 1990.

24. Jen, M. R., J. M. Hsu and D. G. Hwang, "Fatigue Degradation in Centrally Notched Quasi-Isotropic Laminates," *Journal of Composite Materials*, Vol.24. pp. 823-837, 1990.

25. Liu, B. and L. B. Lessard, "Fatigue and Damage-Tolerance Analysis of Composite Laminates: Stiffness Loss, Damage Modelling, and Life Prediction," *Composites Science and Technology*, Vol. 51, pp. 43-51, 1994.

26. Reifsnider, K.L., "Critical Element Concepts for Residual Strength and Life Prediction," Proceedings of the American Society for Composites, pp. 387-403, 1986.

27. Rotem, A. and H. G. Nelson, "Failure of a Laminated Composite Under Tension-Compression Fatigue Loading," *Composites Science and Technology*, Vol. 36, pp. 45-62, 1989.

28. Wolterman, R.L., J. M. Kennedy and G. L. Farley, "Fatigue Damage in Thick, Cross-Ply Laminates with a Center Hole," Composite Materials: Fatigue and Fracture, Fourth Volume, ASTM STP 1156, W.W. Stinchcomb and N.E. Ashbaugh, Eds., American Society for Testing and Materials, Philadelphia, 1993, pp. 473-490.

29. Norman, T. L., T. S. Civelek and J. Prucz, "Fatigue of Quasi-Isotropic Composite Cylinders under Tension-Tension Loading," *Journal of Reinforced Plastics and Composites*, Vol. 11, pp.1286-1301, 1992.

30. Spearing, S. M. and P. W. R. Beaumont, "Fatigue Damage Mechanics of Composite Materials. I: Experimental Measurement of Damage and Post-Fatigue Properties," *Composites Science and Technology*, Vol. 44, pp. 159-168, 1992.

31. Spearing, S. M., P. W. R. Beaumont and M. F. Ashby, "Fatigue Damage Mechanics of Composite Materials. II: A Damage Growth Model," *Composites Science and Technology*, Vol. 44, pp. 169-177, 1992.

32. Spearing, S. M. and P. W. R. Beaumont, "Fatigue Damage Mechanics of Composite Materials. III: Prediction of Post-Fatigue Strength," *Composites Science and Technology*, Vol. 44, pp. 299-307, 1992.

33. Spearing, S. M., P. W. R. Beaumont and P. A. Smith, "Fatigue Damage Mechanics of Composite Materials. IV: Prediction of Post-Fatigue Stiffness," *Composites Science and Technology*, Vol. 44, pp. 309-317, 1992.

34. Hwang, W. and K. S. Han, "Fatigue of Composites - Fatigue Modulus Concept and Life Prediction," *Journal of Composite Materials*, Vol.20, pp. 154-165, 1986.

35. Yang, J.N. and M. D. Liu, "Residual Strength Degradation Model and Theory of Periodic Proof Tests for Graphite/Epoxy Laminates," *Journal of Composite Materials*, Vol.11, p. 176, 1977.

36. Ogin, S.L., P. A. Smith and P. W. R. Beaumont, "Matrix Cracking and Stiffness Reduction during the Fatigue of a $(0/90)_S$ GFRP Laminate," *Composites Science and Technology*, Vol. 24, pp. 23-33. 1985.

37. Thionnet, A. and J. Renard, "An Evolution Equation for Transverse Cracking in Laminated Composites under Fatigue Loading," Rech. Aerosp., Vol. 1, pp. 53-64, 1992.

38. Gamby, D., "A Numerical Model for the Accumulation of Transverse Cracks in a Composite Laminate Subjected to Tensile Fatigue Loading," *Composites Science and Technology*, Vol. 50, pp. 285-291, 1994.

39. Lee, J. R. and F. X. De Charentenay, "Short Holding Time Effect on Fatigue Behavior of Unnotched Graphite/Epoxy Laminates $(\pm 45^o)_{2s}$," *Journal of Composite Materials*, Vol.23, p. 912, 1989.

40. Favre, J.P. and J. C. Laizet, *Journal of Material Science Letters*, 5:31 - 32, 1986.

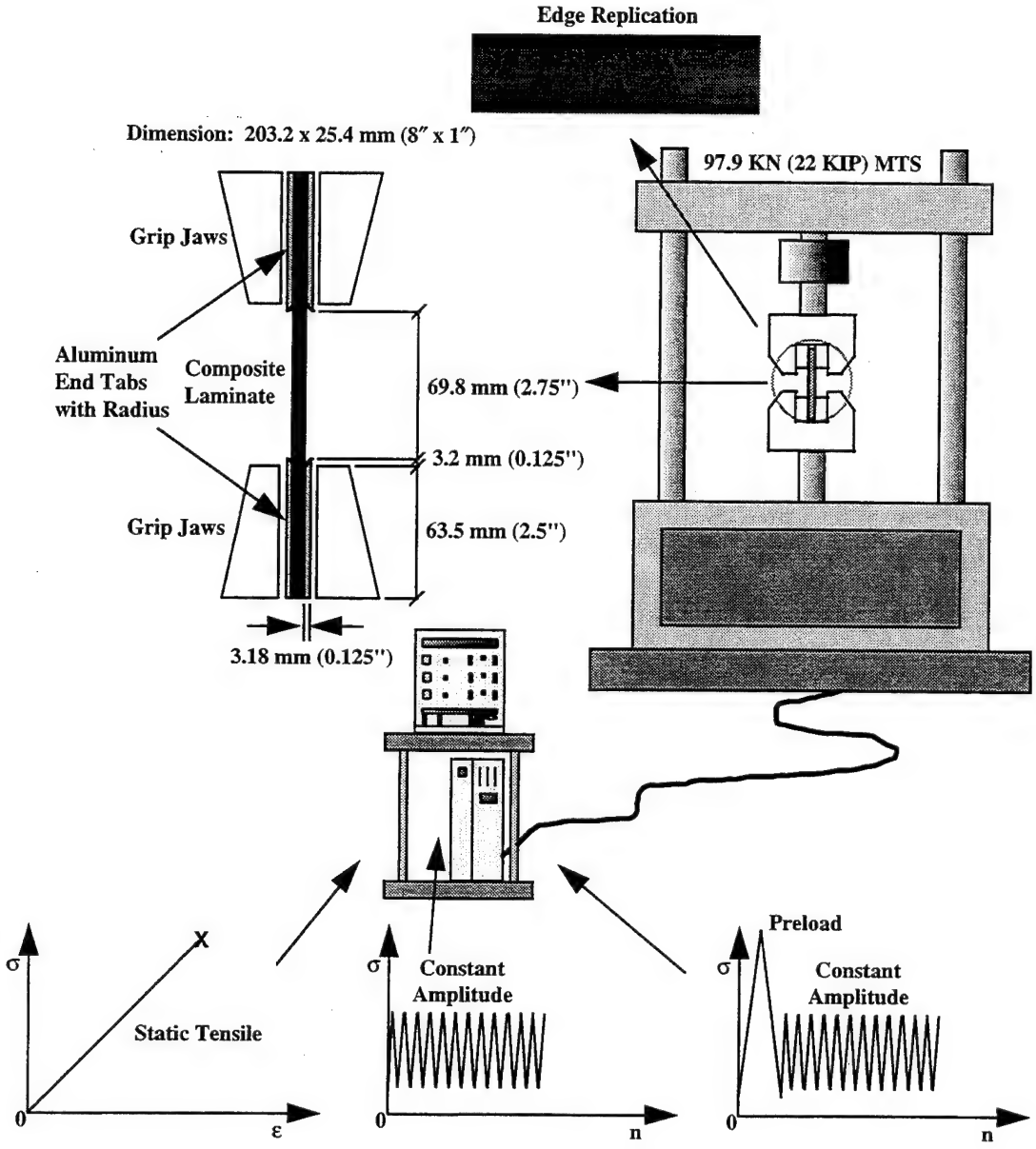

Baseline Fatigue Load Parameters: R=0.1, f=10 Hz

FIGURE 1. SCHEMATIC DIAGRAM OF TEST SETUP

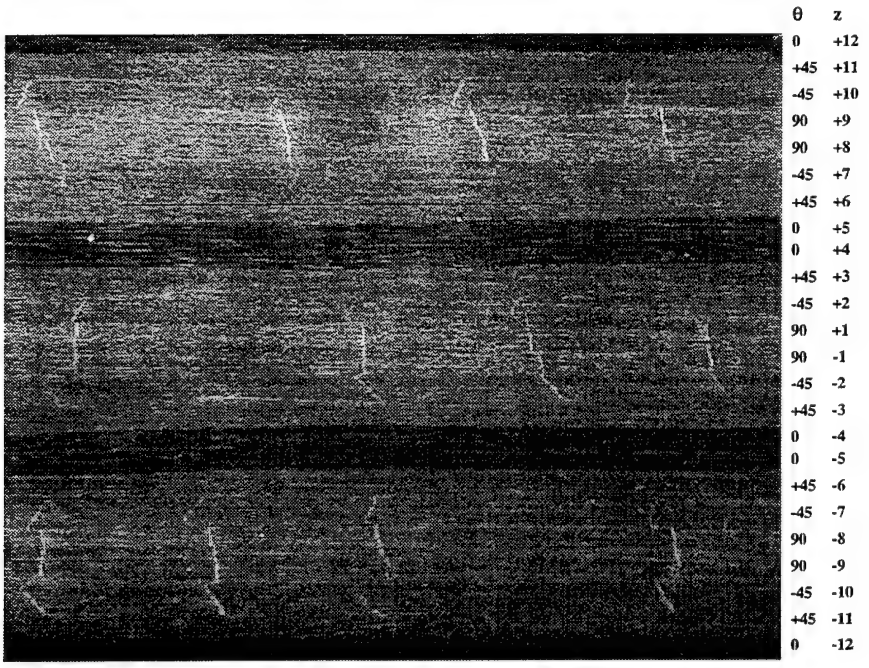

FIGURE 2. PHOTOMICROGRAPH OF $[0/45/-45/90]_{S3}$ LAMINATE SHOWING PLY CRACKS

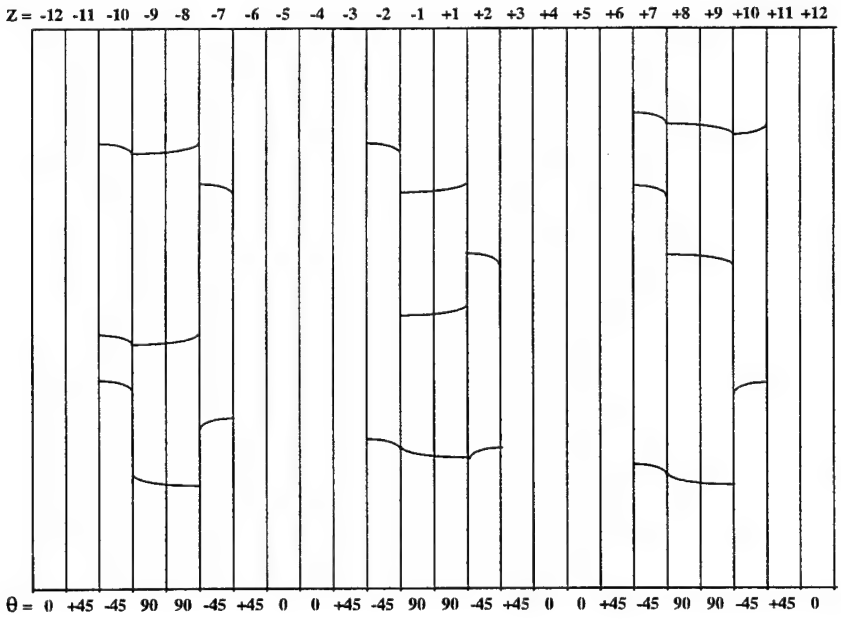

FIGURE 3. LAMINATE LAY-UP AND PLY NUMBERING

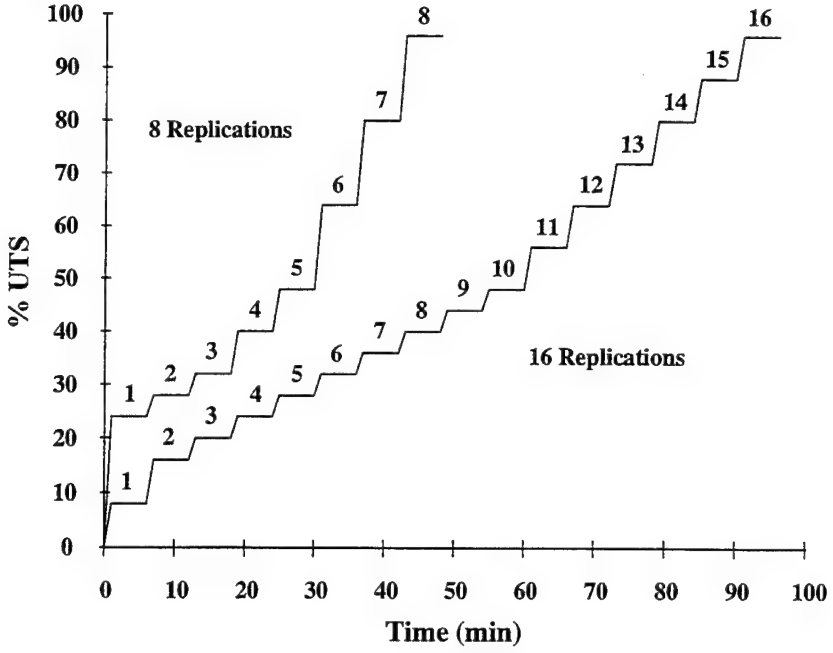

FIGURE 4. LOADING HISTORY FOR 8 AND 16 REPLICATION STATIC TENSILE TEST

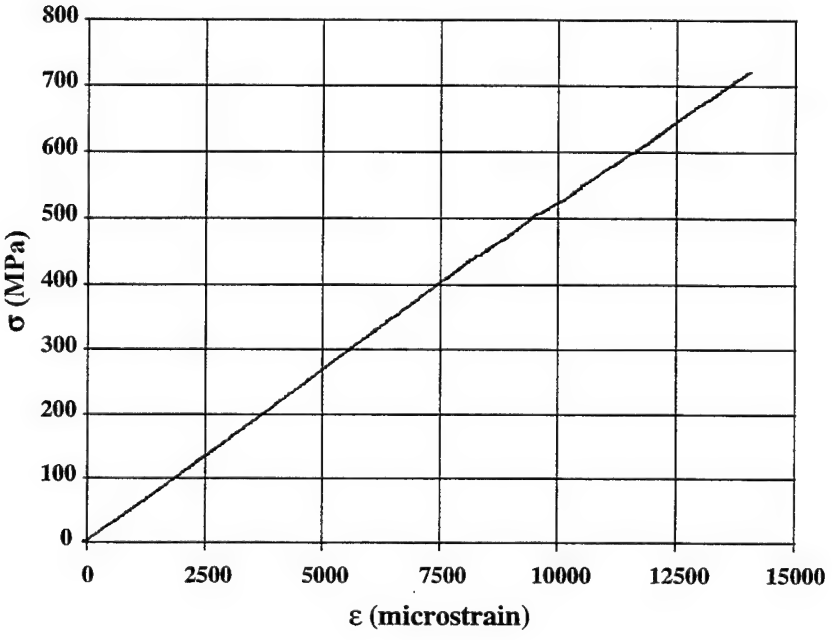

FIGURE 5. STATIC TENSILE STRESS-STRAIN DIAGRAM (25F5)

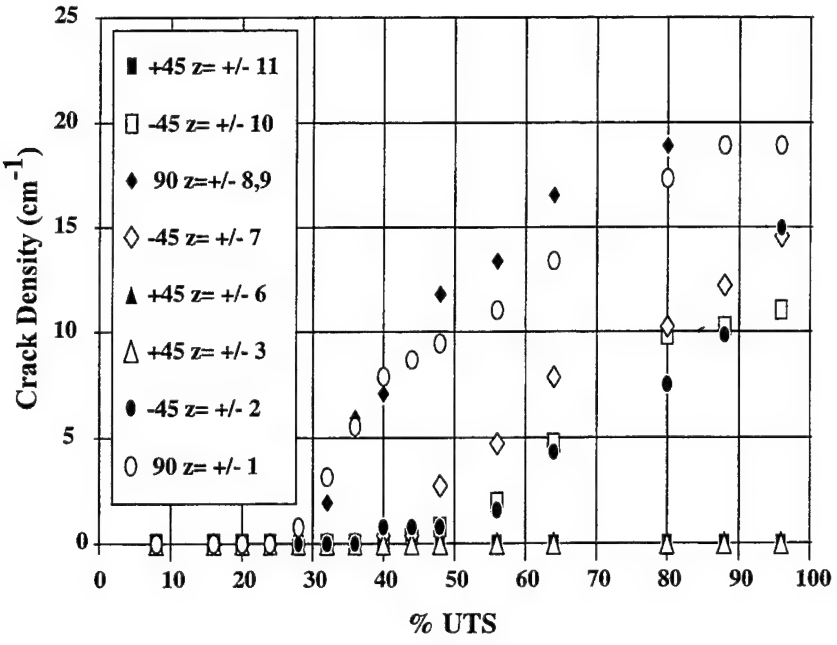

FIGURE 6. DAMAGE ACCUMULATION UNDER STATIC TENSILE LOADING (25F4, 16 REPLICATIONS)

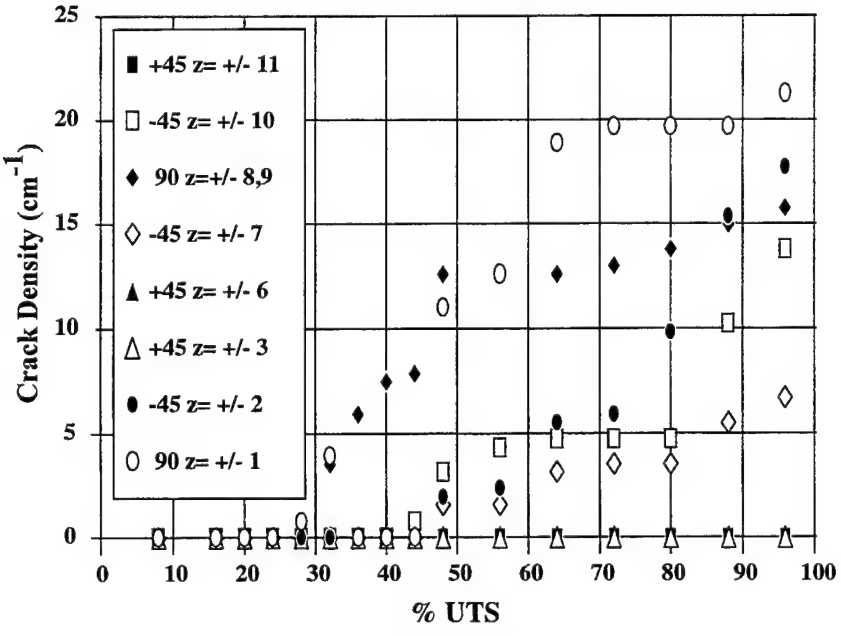

FIGURE 7. DAMAGE ACCUMULATION UNDER STATIC TENSILE LOADING (26E9, 16 REPLICATIONS)

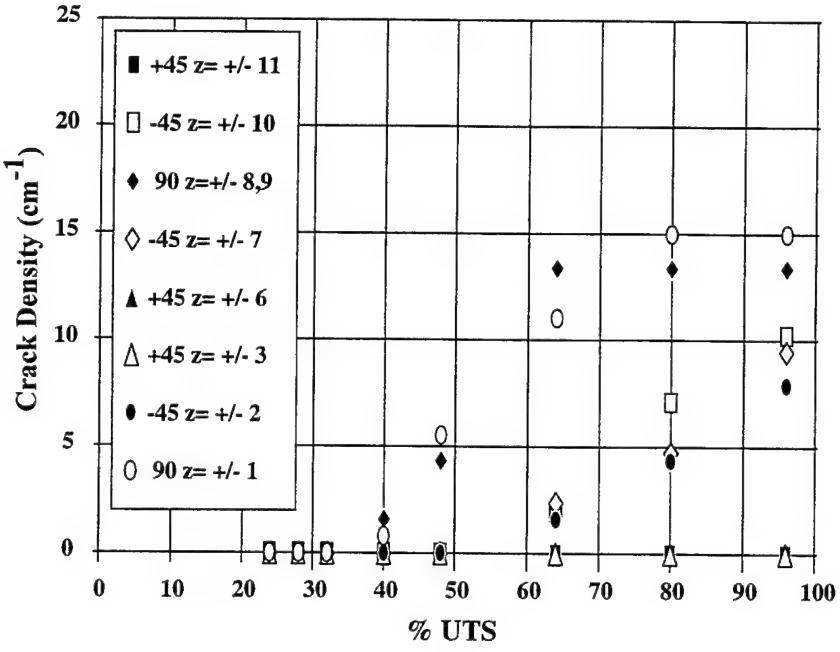

FIGURE 8. DAMAGE ACCUMULATION UNDER STATIC TENSILE LOADING (25B9, 8 REPLICATIONS)

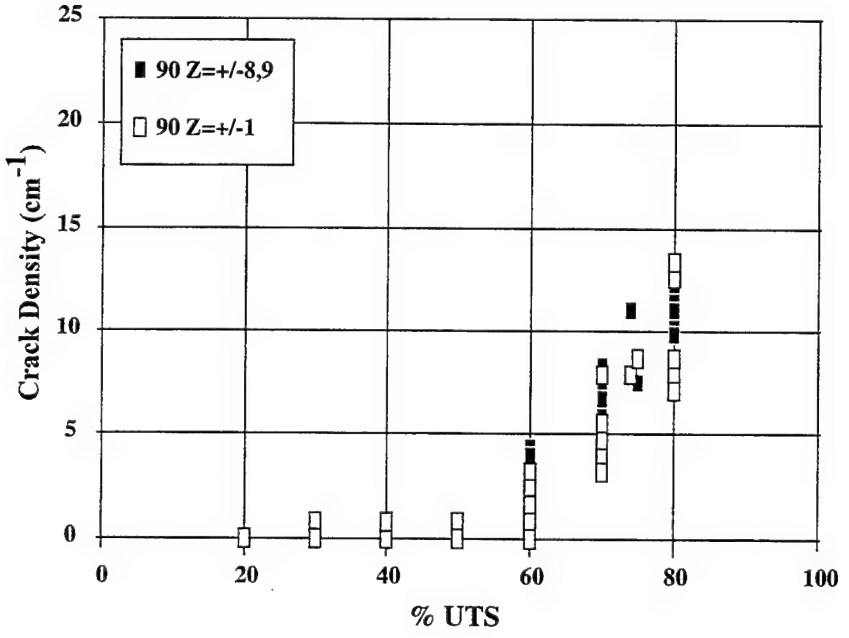

FIGURE 9. FIRST-CYCLE CRACK DENSITY FOR 90° PLIES

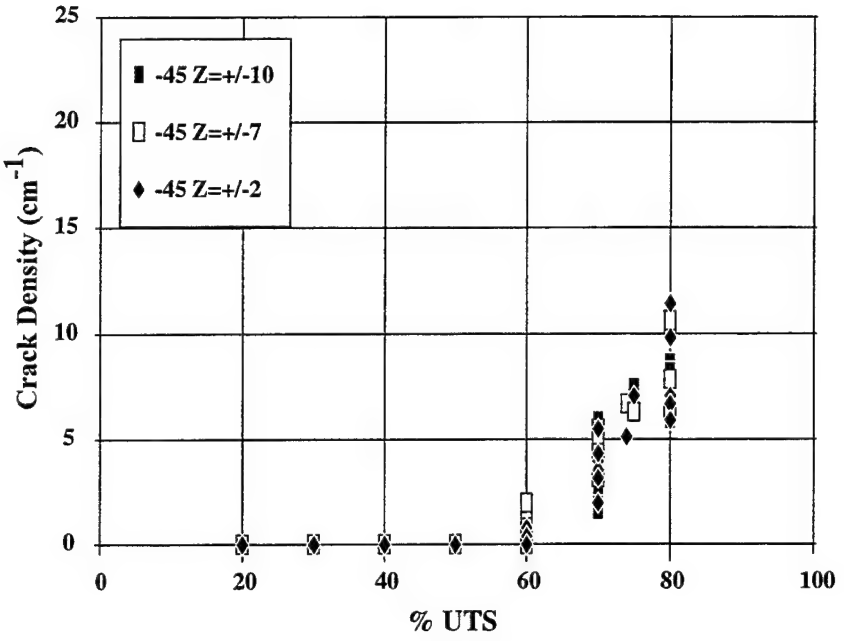

FIGURE 10. FIRST-CYCLE CRACK DENSITY FOR -45° PLIES

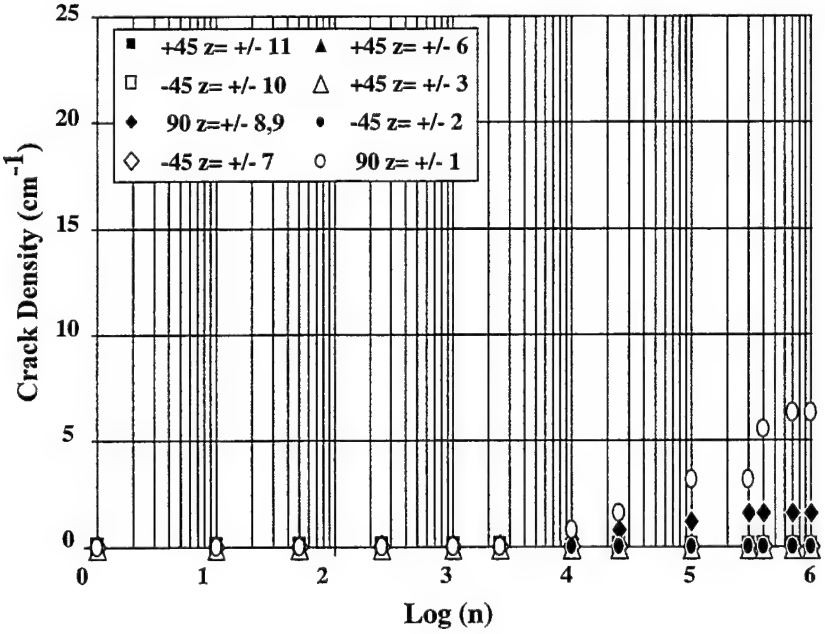

FIGURE 11. PLY CRACK ACCUMULATION UNDER 20% UTS CA T-T LOADING (25F2)

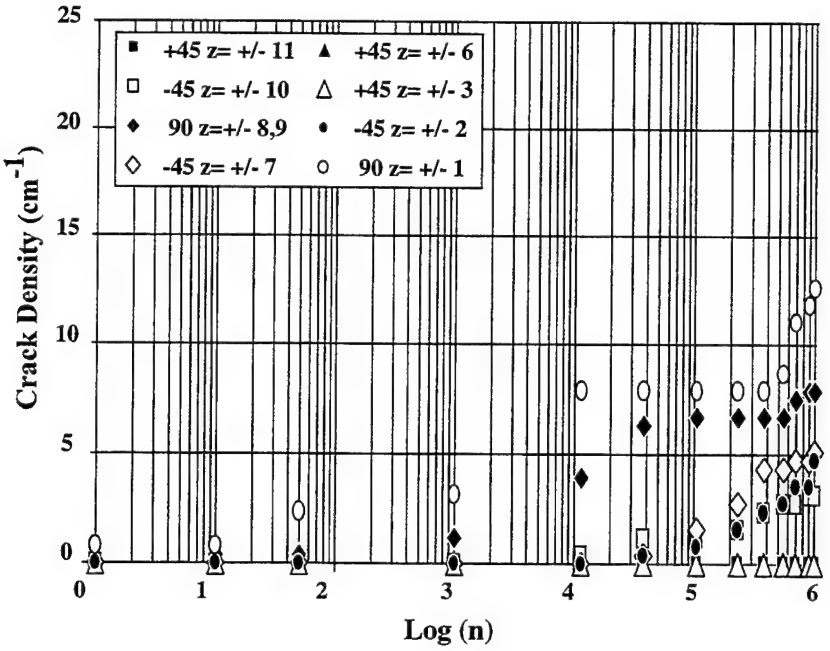

FIGURE 12. PLY CRACK ACCUMULATION UNDER 30% UTS CA T-T LOADING (25C5)

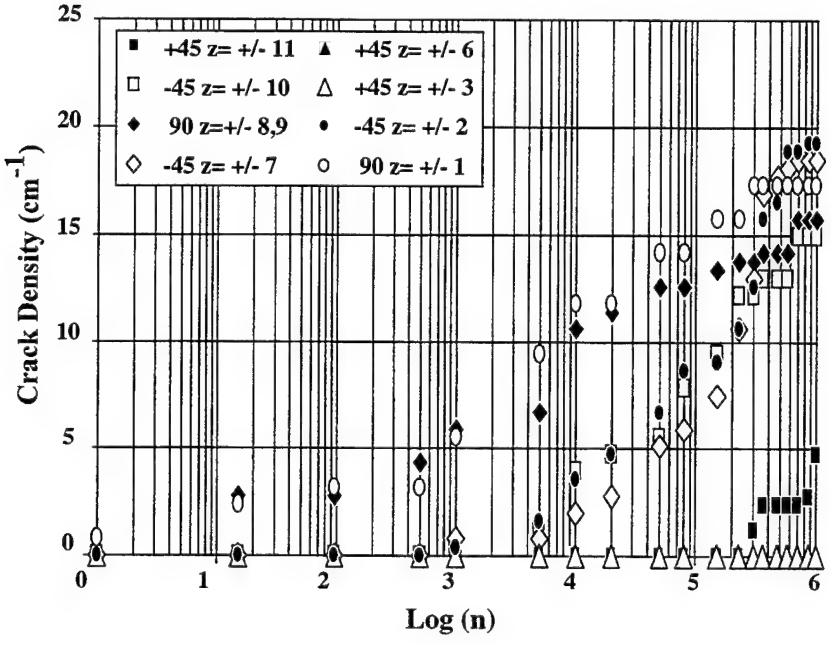

FIGURE 13. PLY CRACK ACCUMULATION UNDER 40% UTS CA T-T LOADING (25D6)

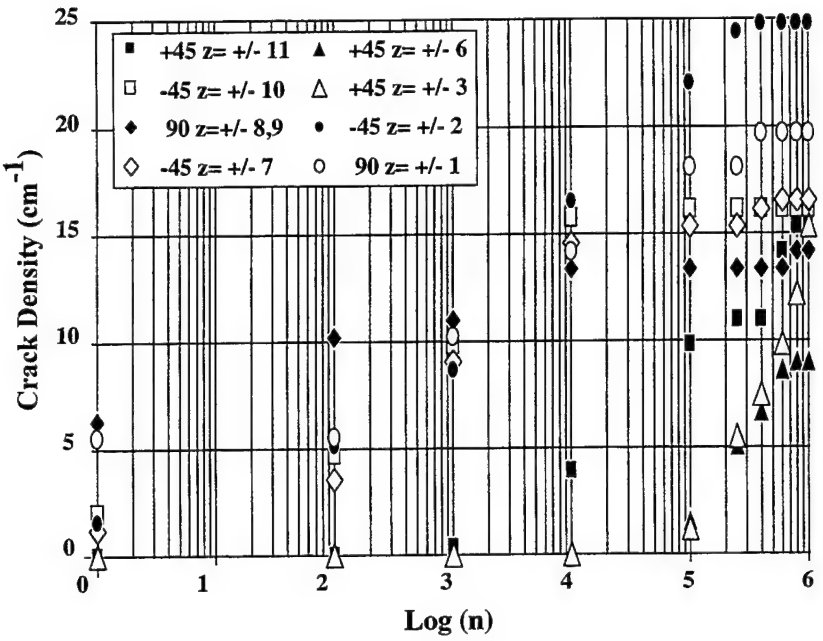

FIGURE 14. PLY CRACK ACCUMULATION UNDER 50% UTS CA T-T LOADING (25C4)

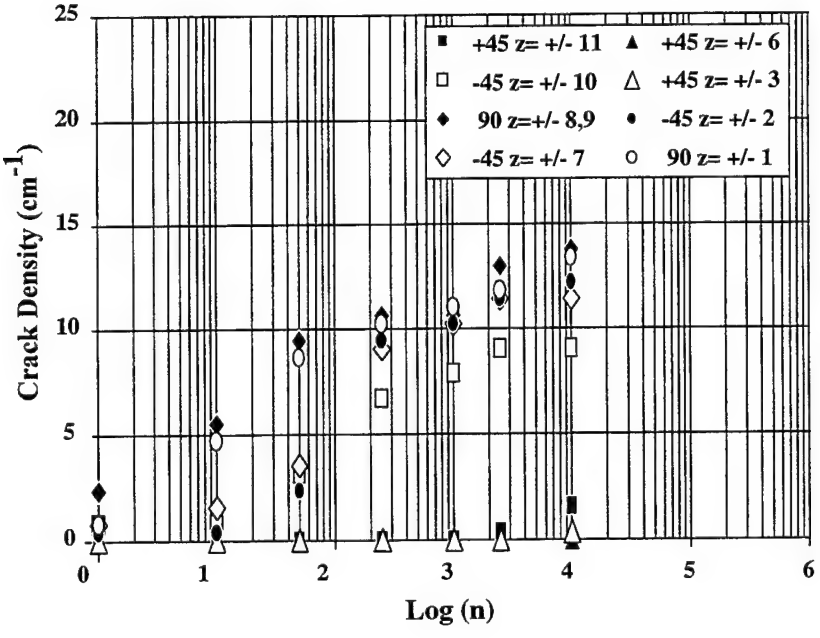

FIGURE 15. PLY CRACK ACCUMULATION UNDER 60% UTS CA T-T LOADING (26B8)

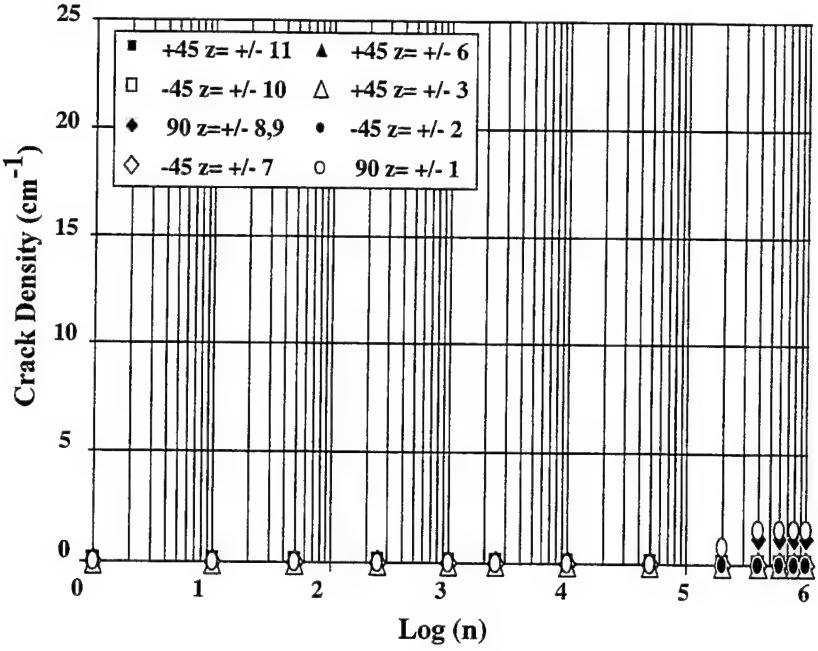

FIGURE 16. PLY CRACK ACCUMULATION UNDER 50% UTS PRELOAD/ 20% UTS CA T-T LOADING (25E2)

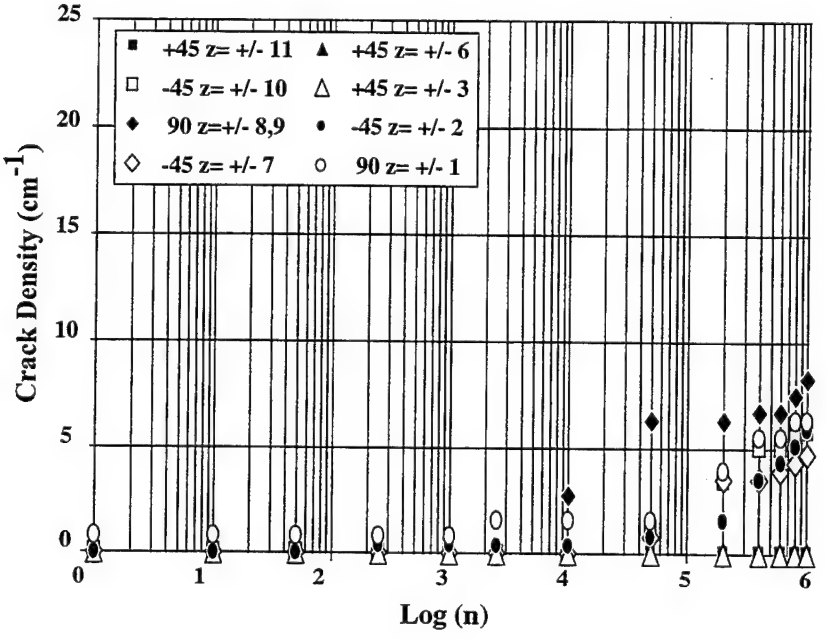

FIGURE 17. PLY CRACK ACCUMULATION UNDER 50% UTS PRELOAD/ 30% UTS CA T-T LOADING (25E11)

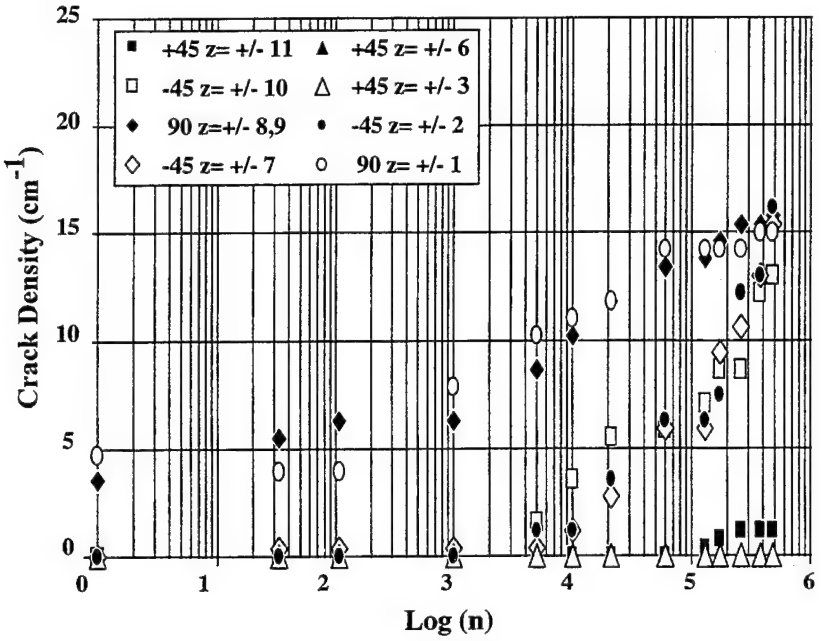

FIGURE 18. PLY CRACK ACCUMULATION UNDER 50% UTS PRELOAD/ 40% UTS CA T-T LOADING (25D8)

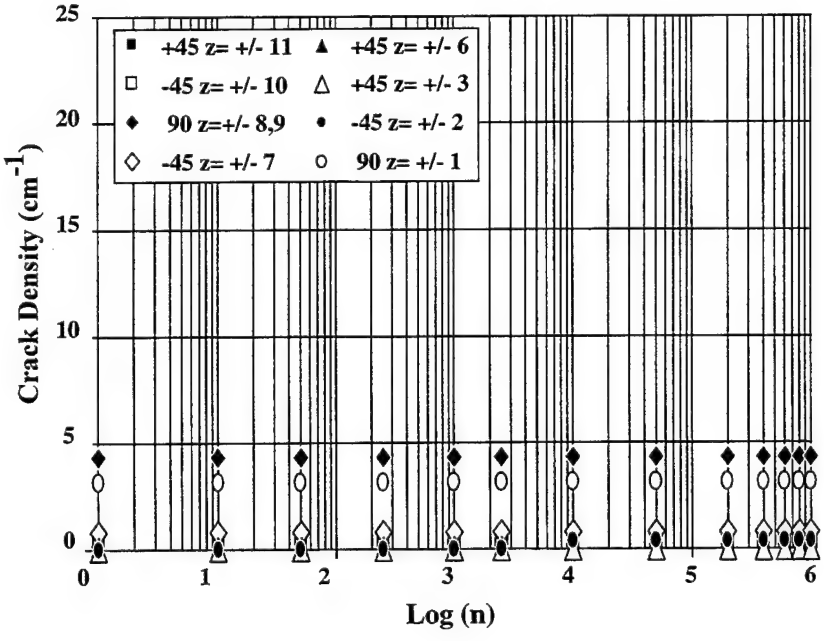

FIGURE 19. PLY CRACK ACCUMULATION UNDER 60% UTS PRELOAD/ 20% UTS CA T-T LOADING (25E7)

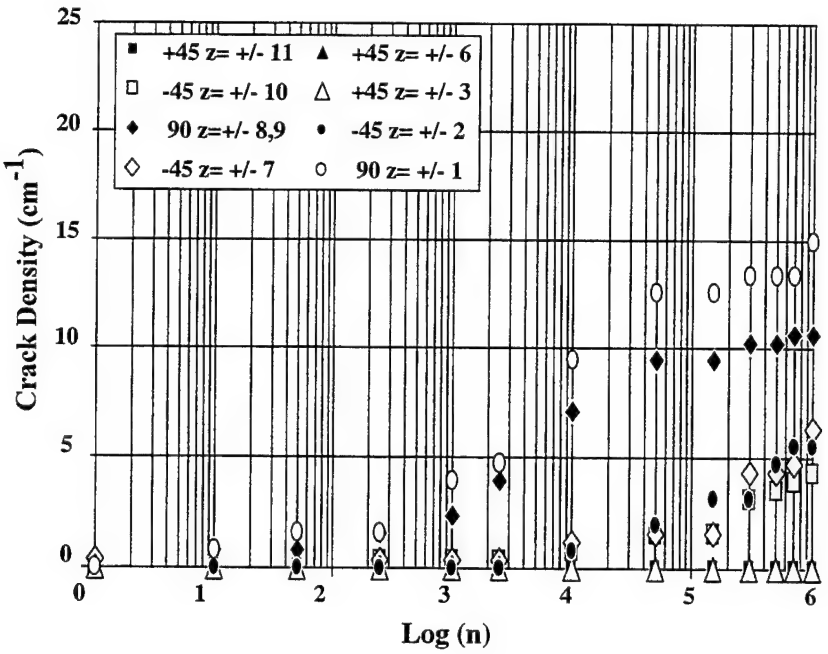

FIGURE 20. PLY CRACK ACCUMULATION UNDER 60% UTS PRELOAD/ 30% UTS CA T-T LOADING (25F1)

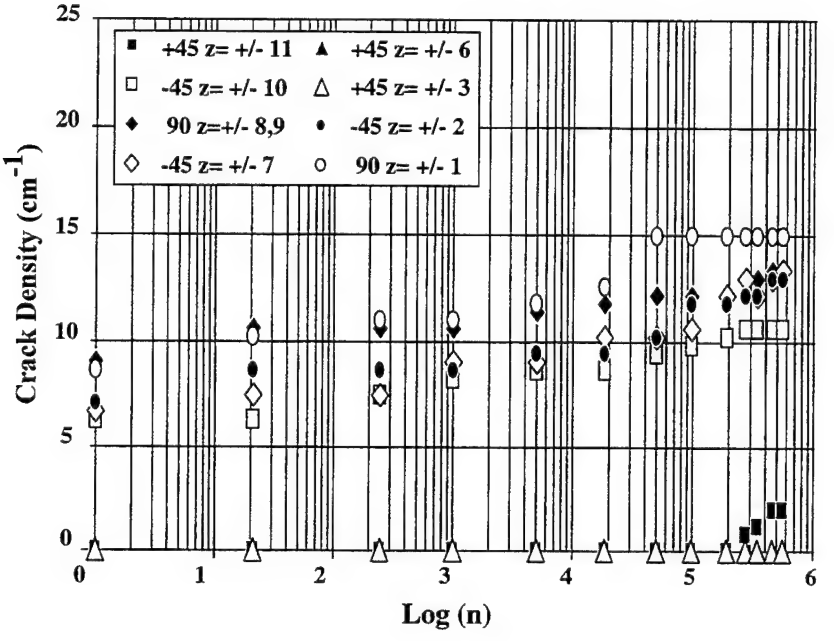

FIGURE 21. PLY CRACK ACCUMULATION UNDER 60% UTS PRELOAD/ 40% UTS CA T-T LOADING (25D5)

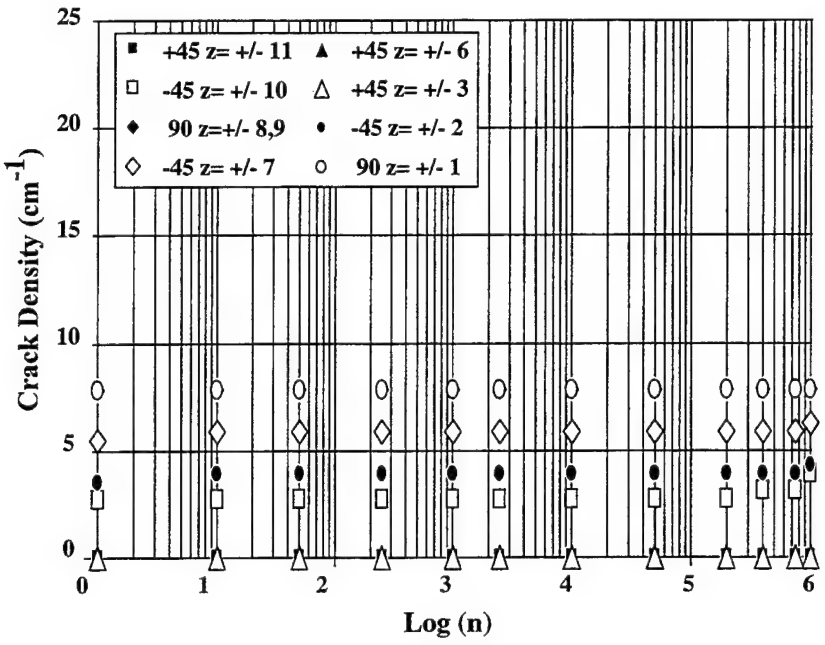

FIGURE 22. PLY CRACK ACCUMULATION UNDER 70% UTS PRELOAD/ 20% UTS CA T-T LOADING (26A11)

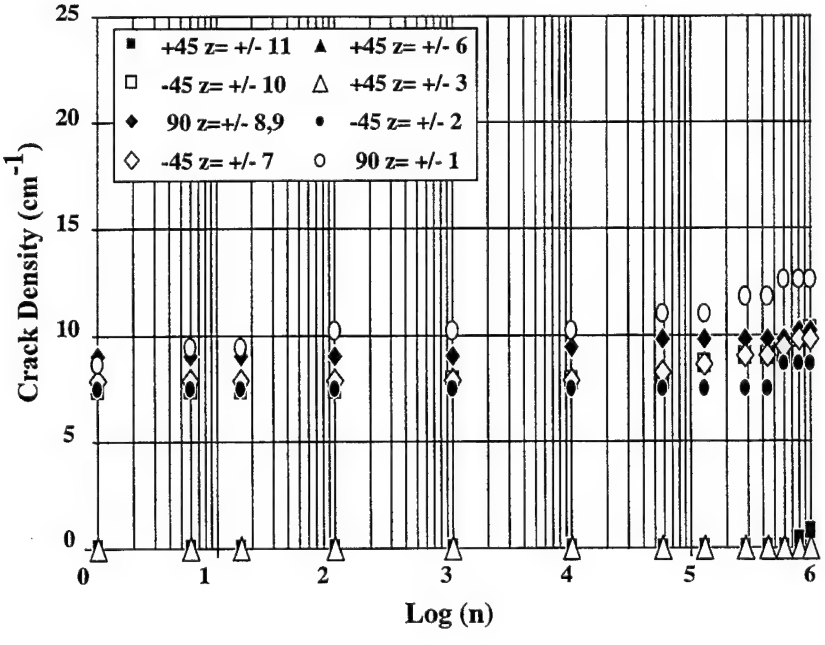

FIGURE 23. PLY CRACK ACCUMULATION UNDER 70% UTS PRELOAD/ 30% UTS CA T-T LOADING (25C6)

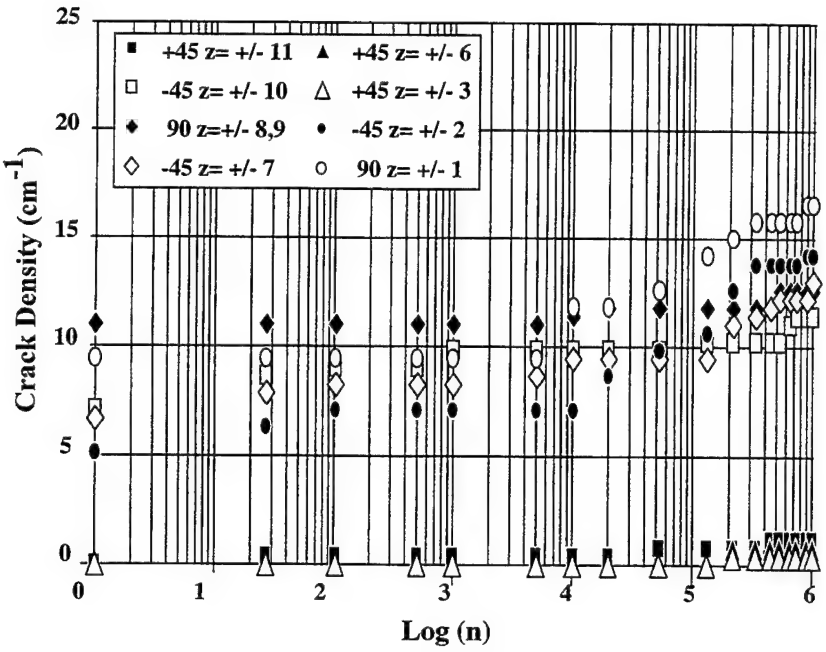

FIGURE 24. PLY CRACK ACCUMULATION UNDER 70% UTS PRELOAD/ 40% UTS CA T-T LOADING (25D4)

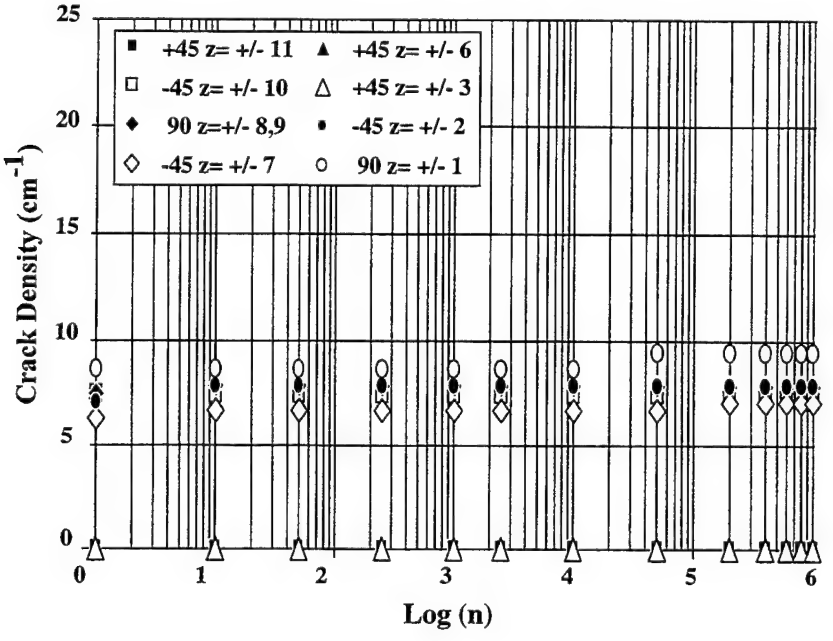

FIGURE 25. PLY CRACK ACCUMULATION UNDER 80% UTS PRELOAD/ 20% UTS CA T-T LOADING (25F3)

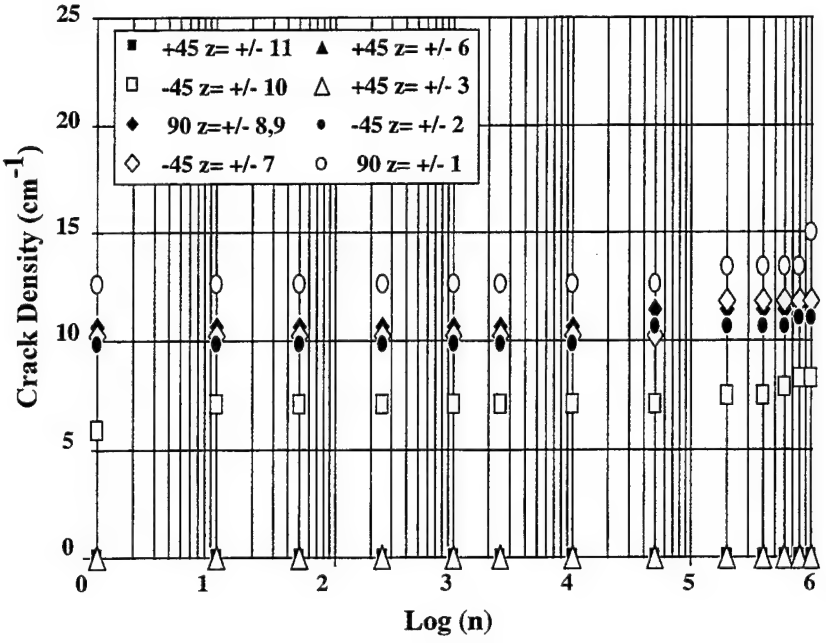

FIGURE 26. PLY CRACK ACCUMULATION UNDER 80% UTS PRELOAD/ 30% UTS CA T-T LOADING (25F6)

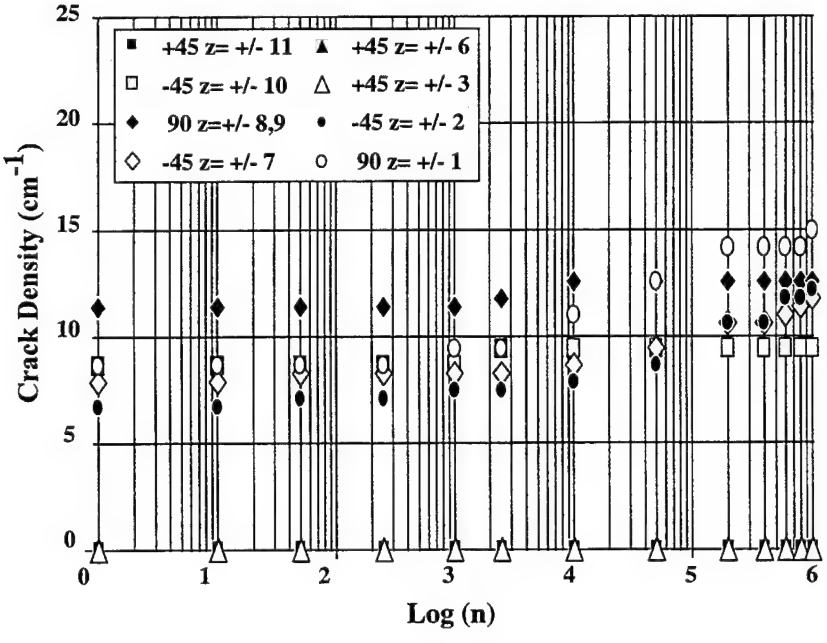

FIGURE 27. PLY CRACK ACCUMULATION UNDER 80% UTS PRELOAD/ 40% UTS CA T-T LOADING (26B2)

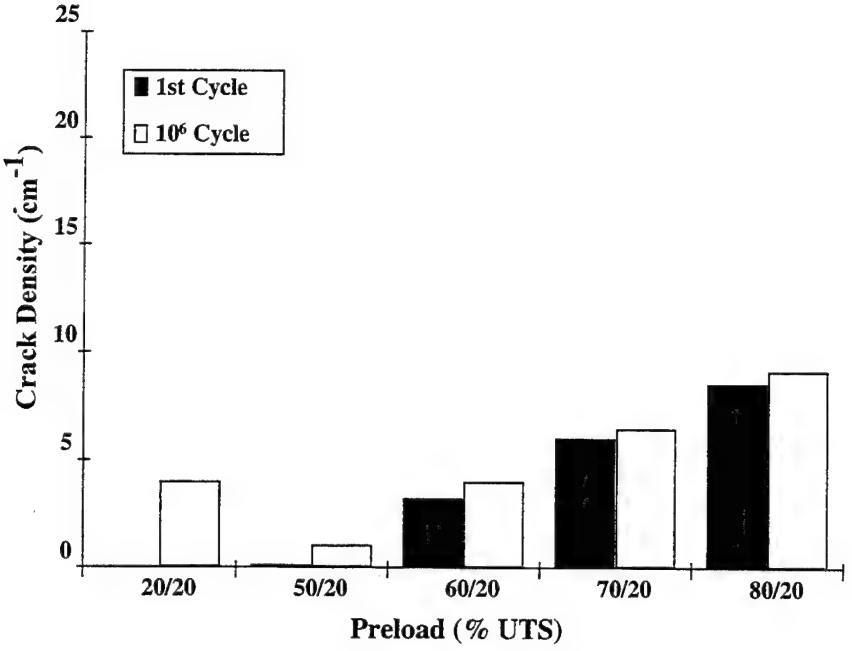

FIGURE 28. 20% UTS FATIGUE CRACK DENSITIES AT 1 AND 10^6 CYCLES VS. PRELOAD FOR 90° PLIES

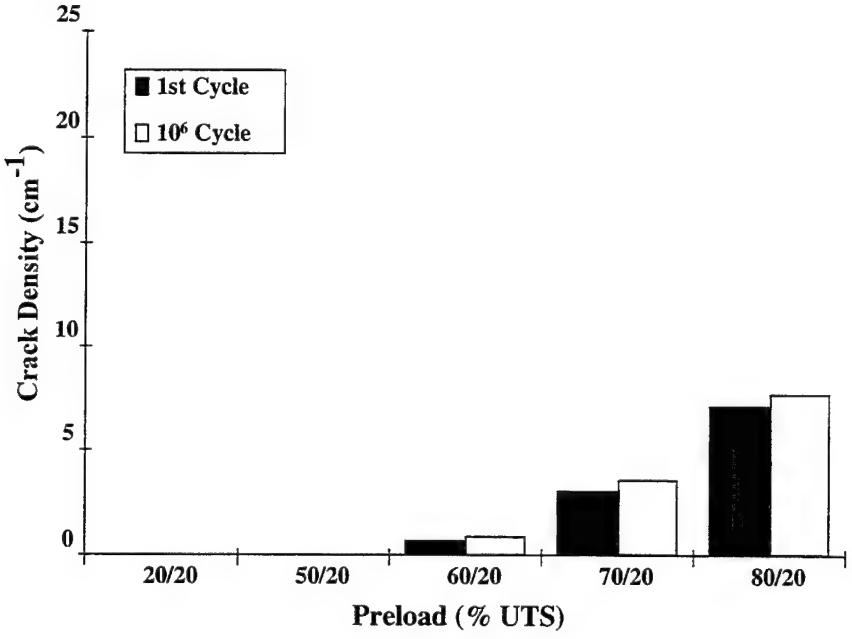

FIGURE 29. 20% UTS FATIGUE CRACK DENSITIES AT 1 AND 10^6 CYCLES VS. PRELOAD FOR -45° PLIES

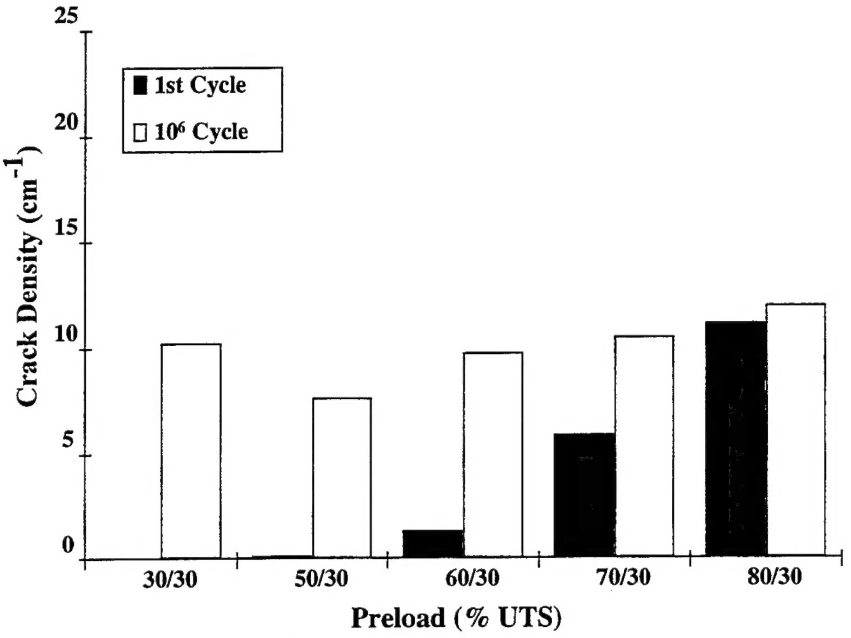

FIGURE 30. 30% UTS FATIGUE CRACK DENSITIES AT 1 AND 10^6 CYCLES VS. PRELOAD FOR 90° PLIES

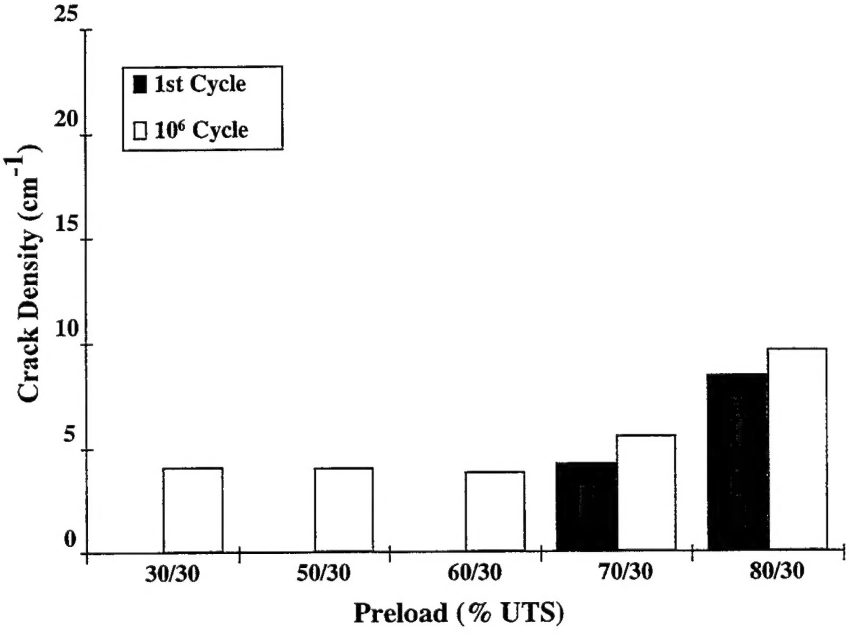

FIGURE 31. 30% UTS FATIGUE CRACK DENSITIES AT 1 AND 10^6 CYCLES VS. PRELOAD FOR -45° PLIES

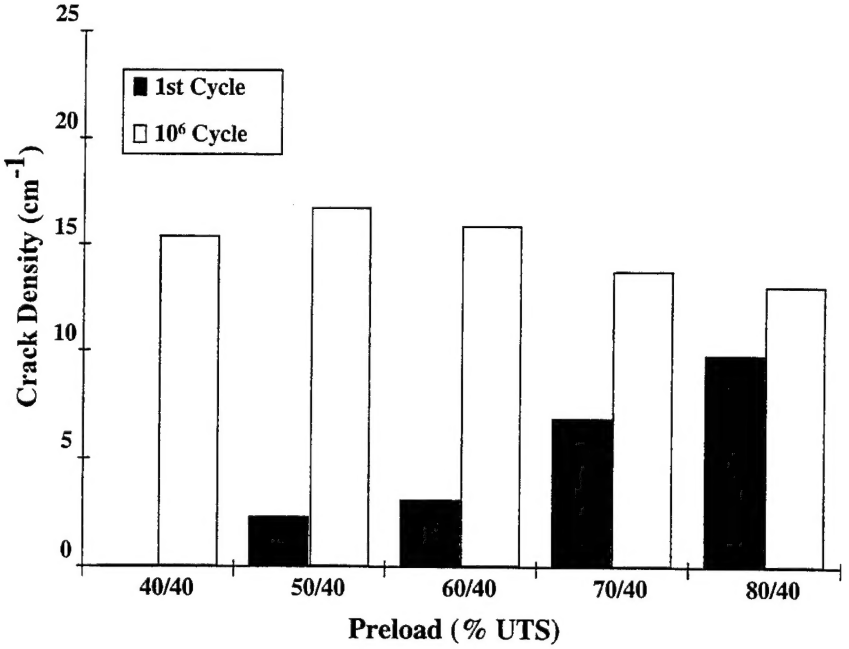

FIGURE 32. 40% UTS FATIGUE CRACK DENSITIES AT 1 AND 10^6 CYCLES VS. PRELOAD FOR 90° PLIES

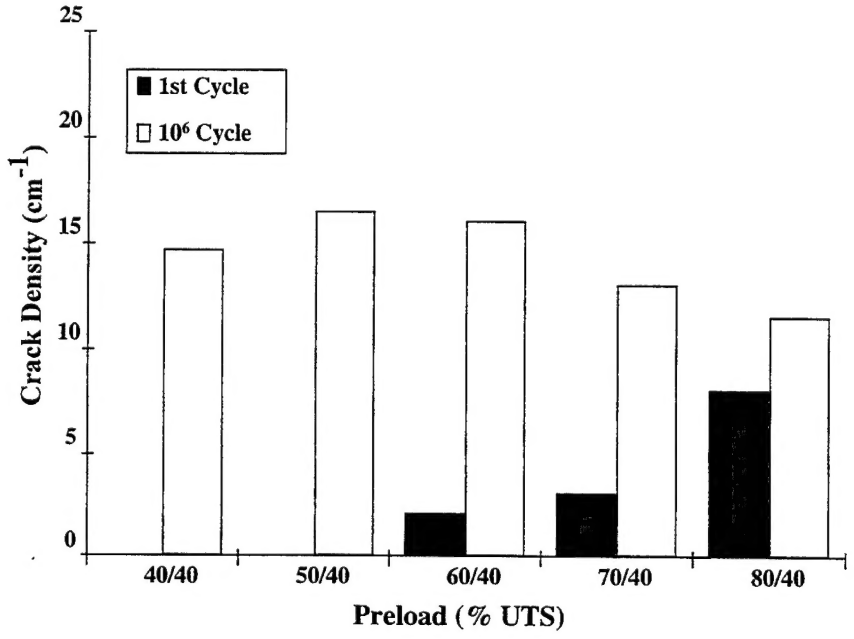

FIGURE 33. 40% UTS FATIGUE CRACK DENSITIES AT 1 AND 10^6 CYCLES VS. PRELOAD FOR -45° PLIES

TABLE 1. TEST MATRIX FOR STATIC AND FATIGUE LOADING

I. Static Tensile Tests

- **Obtain Ultimate tensile Strength (UTS): A**
- **Obtain crack density as a function of load level: B, C**

A. Strain Gaged	**B. 16 Replications**	**C. 8 Replications**			
1. 26B5	1. 26E9	1. 25B9			
2. 26A5	2. 25F4				
3. 25F9					
4. 25F5					
5. 25E5					

II. Constant Amplitude Fatigue

- **R=0.1, f=10 Hz**
- **σ_{max}=20%, 30%, 40%, 50%, 60% of UTS**

A. 20%	**B. 30%**	**C. 40%**	**D. 50%**	**E. 60%**	
1. 25F2	1. 25C1	1. 25D6	1. 25C4	1. 26B8	
2. 26F3	2. 25C5	2. 26C4			
	3. 25E4				

III. Constant Amplitude Fatigue with Preload

- **Preload: 1st Cycle @ R=0.0, f=0.1 Hz, σ_{max}=50%, 60%, 70%, 80%**
- **Constant Amplitude @ R=0.1, f=10 Hz, σ_{max}=20%, 30%, 40%**

50% Preload			**60% Preload**		
A. 20%	**B. 30%**	**C. 40%**	**A. 20%**	**B. 30%**	**C. 40%**
1. 25E2	1. 25E11	1. 25D8	1. 26A4	1. 25F1	1. 25D5
2. 26A10			2. 25E7	2. 26C5	2. 26A7
3. 25E5					3. 25E1
70% Preload			**80% Preload**		
A. 20%	**B. 30%**	**C. 40%**	**A. 20%**	**B. 30%**	**C. 40%**
1. 26F1	1. 25C6	1. 25D4	1. 25F3	2. 25F6	1. 26B2
2. 26A11	2. 26A6		2. 26F9	2. 26F8	2. 26E5
3. 26F7				3. 26E10	

TABLE 2. STATIC TENSILE TEST RESULTS

	σ_{ULT}		ε_{ULT}	E_{11}[1]	
	[MPa]	[Ksi]	[%]	[GPa]	[Msi]
26B5	797.2	115.7	1.49	55.75	8.09
26A5	781.3	113.4	1.44	56.75	8.24
25F9	705.5	102.4	1.33	N/A[2]	N/A
25F5	721.4	104.7	1.41	53.39	7.75
25E5	730.3	106.0	1.39	54.59	7.92
Average	**747.2**	**108.4**	**1.41**	**55.12**	**8.00**
Stand. Dev.	**35.63**	**5.2**	**0.05**	**1.26**	**0.18**
Cov. [%]	**4.77**		**3.67**	**2.29**	

1. Longitudinal stiffness obtained for strain ranging from 0.2% to 1.0% by linear regression, setting y-intercept to be zero.
2. Load voltage vs strain data lost. Only the final load and strain available from previous reports.